

## **Authors response to Editor (part 2)**

We are thankful for your supportive comments and we hope we have successfully addressed your questions and concerns.

### *Specific Comments from Editor*

**Firstly, Table 1 is very enlightening. Could you please confirm for me, are your conclusions about the C sources utilized by the corals based only on sample D03-B1, or do they also use data from other carbonate samples, which elsewhere in the manuscript are also referred to as coral skeleton?**

**Response:** Our conclusions addressing the unlikely use of methane as carbon source by CWCs is based on DNA data (section 3.5) from sample D03-B1 (a necrotic fragment from a living *Madrepora oculata*) and stable carbon isotopes also from sample D03-B1, and from embedded corals in samples D10-R3 and D11-R8. Results concerning stable carbon isotopes are found in section 3.3 (lines 275–304 of revised manuscript; Table 4; Figs. 7 & 9). We have additionally included this information again in Table 1 (lines 737–738 of revised manuscript)

**Secondly, I do not feel that my comment about your proposed biological buffer has been fully answered. I am happy with the statement that 'These microbes may form a biological buffer...', however I am not happy with the stronger statement starting 'This model explains the observed co-existence of ...' I do not feel that other explanations (such as coral tolerance of sulphide etc.) have been fully discussed. Please either moderate and shorten section 4.3 (it would be acceptable if limited mostly to the first paragraph), or provide substantial additional argument, support from the literature, and description of patterns in your own data which support the hypothesis.**

**Response:** we fully understand your concerns and revised the chapter 4.3 accordingly, essentially following your suggestions to moderate and shorten the chapter. We furthermore tried to emphasize that the proposed “biological buffers” appear to be a further, additional ecological factor that is relevant for CWC development in the study area. We also stress that CWCs have certain ecological capabilities that may allow them to thrive at seepage-influenced localities and provide relevant references. Finally, we tried to stress that the geographical extent of these biological buffers has to be further evaluated (i.e., local vs. regional vs. global relevance). In combination, our changes hopefully make clear that the biological buffers are an important aspect for CWCs in seepage-influences environments, but that this by no means exclude other influences such as ecological capabilities of the corals or other environmental factors.

## Authors response to Editor

*Dear Dr Rincón-Tomás*

*Thank you for submitting your revised manuscript. I would like to request some additional changes, many of which aim to ensure that the reasoning you provide in response to reviewer comments is actually included in the manuscript discussion. Please could you therefore undertake further revisions to accommodate the comments below.*

*Best regards,*

*Clare Woulds*

**Authors:** we appreciate your constructive comments on our manuscript. We are also thankful for the extra time you have given us to improve the manuscript and address successfully all discussion points.

**You mention twice that the aim of the study was to ‘...address the linkage between CWCs and present day formation of MDACs.’ The fact that two reviewers have questioned the study objectives / hypotheses supports my feeling that the phrase ‘address the linkage’ is not sufficiently explicit. Please re-phrase your aim and research questions in plainer language, and state the hypothesis that you were testing.**

**Response:** we have now added some more sentences indicating the hypothesis of our study, which to prove if CWCs are non-chemosynthetic organisms or they rather harbor chemosynthetic symbionts which allow them consuming some of the seeped fluids.

**Please ensure that the answer to reviewer 2 point 19 is included in the discussion, with appropriate acknowledgement that the tissue you analysed was not living biomass (i.e. coral polyps), that analysis of such live tissue would be required to draw firm conclusions that methane C was not a major dietary C source, and stressing that the conclusion that can be drawn is that methane C was not a major C source during building of the exoskeleton. I recognise your point that if the corals were using methane derived C, then when it was metabolised some of it may be incorporated into the exoskeleton. However, the lack of (much) evidence for this is a rather tenuous way of drawing a conclusion about how the corals fulfilled their metabolic needs.**

**Response:** We have added more information addressing this issue in the discussion, between lines 391–394 and 409 from the revised manuscript. We specify our analyzed sample is a “necrotic part of a living *Madrepora oculata*” in line 396.

**Likewise, please include the response to reviewer 2 point 20 in the discussion.**

**Response:** Response to reviewer 2, point 20 have been included in the results (lines 262–263) and in the foot of Figure 6 (lines 812–813). We have considered that this information is better adapted to those sections, rather than in the discussion section.

**Please ensure that all responses to reviewer 3 are also included in the text.**

**Response:** done.

**Line 53 – ‘Supports’ should be replaced with ‘suggests’.**

**Response:** done.

**Please add a table, referred to in the opening paragraphs of the method section (therefore Table1), detailing study site lat and long, depths, and number of samples of each type collected. Please also indicate the number of replicate samples of each type collected at each location.**

**Response:** A table (now Table 1) has been added to remark and clarify the sampling sites, as well as the type of samples recovered from those sites. Since those samples were unique, there are no replicates of the original samples. Some analysis (e. g. stable isotopes, environmental DNA) do use different replicates from the same sample in order to accomplish stronger results, and those methods can be found in the material and methods section.

**Please add identification of internal and external standards used for GC and isotopic analyses, as well as indications of precision for quantification of lipids and isotopic ratios.**

**Response:** in case of stable isotopic analyses of the carbonates, accuracy and reproducibility were checked through the replicate analysis of a standard (NBS19), and the reproducibility was better than 0.1 ‰. This information is already provided in the methods section.

In case of stable carbon isotopic analyses of organic compounds, CO<sub>2</sub> of known stable carbon isotopic composition was used for internal calibration. This information is already provided in the methods section. The reference CO<sub>2</sub> was calibrated with a standard (IAEA600). Standard deviations of duplicate sample measurements were better than 1.0 ‰. We included this information into the method section.

Lipid biomarkers were not quantified, therefore no standard was needed.

**Line 413-end of discussion. Your hypothesis regarding a biological buffer requires further discussion and possibly evidence. The two questions that occur to me are: 1) Is the presence of sulphide and methane normally prohibitive to the existence of CWCs? At what concentrations do they become problematic? Sulphide is of course toxic at certain concentrations, but non-chemosynthetic ‘normal’ or ‘background’ benthic fauna can and do inhabit sites with some level of sulphide flux (see Bell et al. 2016, *Frontiers in Marine Science*), and methane is even less of a problem. 2) Do you have evidence (i.e. porewater and bottom water methane and S<sup>-</sup> concentrations) to show that bacterial activity does indeed lead to reductions in sulphide concentrations such that they allow colonisation by CWCs? I’d suggest that there is another explanation, which is that CWCs are tolerant to some extent of sulphide**

**and methane fluxes, however sulphide and methane may cause some degree of stress, which may at least partially explain the poor health (low abundance of living material) that you observed.**

**Detail response to “1) Is the presence of sulphide and methane normally prohibitive to the existence of CWCs? At what concentrations do they become problematic? Sulphide is of course toxic at certain concentrations, but non-chemosynthetic ‘normal’ or ‘background’ benthic fauna can and do inhabit sites with some level of sulphide flux (see Bell et al. 2016, *Frontiers in Marine Science*), and methane is even less of a problem”:** We agree that non-chemosynthetic fauna is able to live in conditions where sulfide and methane fluxes are present in “some level”. Interestingly, when seepage of methane and/or sulfide occurs, there is normally chemosynthetic-fauna related to this seepage, which are actually “buffering” the harmful “levels” that could affect those non-chemosynthetic fauna if they would not feed on the seeped fluids. As we observed in Fig. 12, A, which represents the active pockmark found in the Al Gacel MV (Fig. 5), CWCs are living in an active pockmark and actually colonizing a currently-formed AOM carbonate. Furthermore, methane is indeed not toxic for CWCs, but its emission decreases pH and complicates carbonate precipitation (which affects CWCs like scleractinians).

**Detailed response to “2) Do you have evidence (i.e. porewater and bottom water methane and S-concentrations) to show that bacterial activity does indeed lead to reductions in sulphide concentrations such that they allow colonisation by CWCs? I’d suggest that there is another explanation, which is that CWCs are tolerant to some extent of sulphide and methane fluxes, however sulphide and methane may cause some degree of stress, which may at least partially explain the poor health (low abundance of living material) that you observed”:** we have now included S- and Fe values obtained from pore-water and seawater samples (see section 2.2.1 and lines 269 – 274 of new revised manuscript). S- and Fe values in the pore-water are higher than those from the bottom seawater, which indicates its consumption. This can be explained by the observation of framboidal pyrite inside the carbonate D10-R7 (Fig. 8 C–D), as well as environmental bacterial DNA sequences which indicate the presence of sulfide-oxidizing bacteria. Furthermore, ROV images also indicate the presence of siboglinid worms that also consume this sulfide.

## **Authors response to Referee n° 1**

We are thankful for the constructive and helpful comments that have helped us to improve our manuscript. We are aware that the manuscript holds a high amount of data which can be difficult to follow at some points and tried to keep it as concise as possible. We considered all comments carefully and modified and followed most of the suggestions.

### *Specific Comments from Referee n° 1*

**2) The introduction reads well. One question is whether you have a testable hypothesis. Are you trying to ask whether the corals are fueled by fluids versus scavenging from currents. How are you going to distinguish between mechanisms?**

**Response:** the aim of the study is to address the linkage between CWCs and present day formation of MDACs in the Pompeia Province. For this purpose, we combined analyses of ROV images, geophysical data and sample materials. For instance, we analyzed  $\delta^{13}\text{C}$  signatures of coral skeletons to evaluate whether these organisms were directly relying on  $\text{CH}_4$ . We found that the coral skeletons exhibited significantly higher  $\delta^{13}\text{C}$  values than the co-occurring AOM-derived carbonates, thus not supporting  $\text{CH}_4$  as important carbon source. Rather, the corals were feeding on material suspended in currents.

**3) In the methods please add section in which you describe the Experimental Design. How many samples were collected and from where? The descriptions of the laboratory methods are okay. However, I have no idea if you sampled thoroughly enough.**

**Response:** we included more detailed information on our sample strategy and study design in the material and methods section.

**4) In Table 2, will readers know what Identifier means? I realize that the numbers correspond to pictures in the figures. However, it is very confusing to have to put the figure next to the table to interpret the data in the table. There must be a better way to present the data.**

**Response:** done. We replaced “Identifier” by “Identification number in Fig. 7”. In Addition, we added an additional column to the table in which we provide information on the analyzed material.

**5) Rather than using code numbers for the sampling sites, it would help readers if you used descriptive names, such as ‘active seep’, etc.**

**Response:** done. We have revised the use of code numbers throughout the manuscript.

**6) Although amplicon sampling for microbial group is okay. Do you have evidence for microbial growth and activity? Perhaps in the discussion indicate which samples come from fresh material and are likely to have fresh DNA versus samples in which the DNA could be old and preserved. I realized this is inferred by looking at the pictures, but again this is a convoluted way to present a story.**

**Response:** we have improved the information concerning the DNA material related to each sample in the manuscript, and we have specified the type of sample from which the DNA has been extracted (lines 180–183 in the revised manuscript). Furthermore, we added some extra information in Fig. 11 to clarify and

remain the type of sample. DNA analyses cannot conclude if DNA is “old” or “fresh”, but we can estimate (together with other analyses) if the sample used for this analysis is fresh or not. but we can infer this by assessing the relative age and preservation of the analyzed sample. For instance, an AOM-derived carbonate recovered from an active pockmark (sample D10-R7) exhibits more DNA of AOM-related microorganisms (ANME and SRB) than oxidized AOM-derived carbonates recovered from regions that are currently not affected by seepage (sample D10-R3).

**7) I suppose the model is okay. However, again a better presentation of the data might lead readers to the conclusion rather than relying on the author’s story.**

**Response:** done. We have modified the last paragraph of the section 4.3. for a better understanding of our model (lines 438–445 in the revised manuscript).

*Technical Comments from Referee n° 1*

**1) Line 19: consider saying, ‘rate a seepage via focused, scattered, diffused, etc.’**

**Response:** done. We revised the sentence to “the type of seepage such as focused, scattered, diffused or eruptive”.

**2) Line 34: change ‘which’ to ‘that’.**

**Response:** done.

**3) Line 36: change to ‘typically, they thrive, etc.’**

**Response:** done.

**4) Line 45: change ‘ecological’ to ‘environmental’ and ‘are discussed to control’ to ‘influence’.**

**Response:** done.

**5) Line 51: delete ‘e.g.’.**

**Response:** done.

**6) Line 53: change ‘e.g.’ to ‘for example’.**

**Response:** done.

**7) Line 65: delete ‘i.e.’ and the parentheses. The text is not an example rather it is the description of ‘coral graveyards.’**

**Response:** done.

## **Authors response to Referee n° 2**

We are thankful for your constructive feedback and the helpful comments. We have considered and addressed your suggestions carefully, and almost all have been followed in the revised manuscript.

### ***Detail Comments from Referee n° 2***

**1) Line 1. Title. The text after the hyphen: ‘living on the edge’ is unnecessary and adds nothing to the title. What edge? I suggest removing this.**

**Response:** we would like to keep the text “living on the edge” to emphasize that hydrocarbon-rich seepage has both advantages and disadvantages for cold-water corals growth.

**2) Lines 26-27. Abstract Delta C13 values of the coral skeletons (see below)**

**Response:** see discussion on reviewer comment n° 19 below.

**3) Line 31. Abstract. Suggest ‘seeping’ rather than ‘seeped’ fluids.**

**Response:** done.

**4) Line 61. Suggest ‘In addition’ to replace ‘On the other hand’, as this is not a contrasting observation.**

**Response:** done.

**5) Line 76. ‘Englobes’ is not an English word. Seems like a transliteration of ‘encompasses’.**

**Response:** done.

**6) Line 128. Don’t start sentence with a number – spell it out.**

**Response:** done.

**7) Line 152. Can the authors give a little more detail of the nature of the samples used for the DNA work. Are these MDACs?**

**Response:** done. We now provide more information on the nature of the samples (lines 182–185 in the revised manuscript).

**8) Lines 192-195. The background information about the Gulf of Cadiz isn’t really results and would go better at the start of section 2.**

**Response:** we agree that the background information of the Gulf of Cádiz is not part of results. However, the Pompeia Province region, which our study is focused on, has not been described in detail so far. We here provide the first description of geological structures in this area (Southern and Northern Pompeia Coral ridges, Cold-water Coral Mounds Fields), including novel data (e.g., bathymetry, seismics). For this reason, we consider it appropriate to report these findings in the results sections.

**9) Line 241 and other places. It’s quite difficult at the moment to correlate the isotopic**

**data in Table 2 with the sample points in Figure 7, because the specimen images in Figure 7 are not quite large enough to distinguish samples of authigenic carbonates from embedded coral skeletons. Therefore, could the authors add a column into Table 2 that makes it clear what the samples are for each of the isotopic data points, e.g. authigenic carbonate or coral skeleton.**

**Response:** done. One more column has been added in Table 2 as proposed, indicating the type of samples from which stable isotopic analyses are.

**10) Line 253. Replace ‘stems’ with ‘comes’.**

**Response:** done.

**11) Line 254. In the figure the ‘worms’ look like serpulid worm tubes. Is this so? In which case please add this information.**

**Response:** done.

**12) Line 291. Replace ‘On the contrary’ with ‘In contrast’.**

**Response:** done.

**13) Line 296. Spell out ‘2D’ at start of sentence.**

**Response:** done.

**14) Line 305 and elsewhere. What is ‘dripping-like’ seepage? This isn’t a description I recognize, so it would be helpful if the authors specify what this means.**

**Response:** done. “Dripping-like refers to intermittent bubbling fluids” (lines 342–343 in the revised manuscript).

**15) Line 317. Suggest ‘data’, rather than ‘evidences’.**

**Response:** done.

**16) Line 330. I’m unclear where is being referred to here.**

**Response:** removed.

**17) Line 332. ‘appear’, not ‘appears’, as preceding diapirs is plural.**

**Response:** done.

**18) Line 339. Typo. Angle not angel.**

**Response:** done.

**19) Lines 346-354. The authors here suggest that the seawater-like values of the delta C13 from the dead scleractinian skeletons and those embedded in the MDAC show that the corals do not use**

methane as a food source, either directly or through symbionts. The authors need to be careful here, because some seep organisms that demonstrably do use methane (and sulfide) from seep fluids for food via endosymbionts produce carbonate skeletons that also have seawater-like delta C13 signatures. I am referring here to vesicomid and bathymodiolin bivalves, that sequester seawater bi-carbonate ions to produce their shells. Using this model, having seawater-like delta C13 values in the coral skeletons does not prove that these animals do not use chemosynthetic food sources at the site. Really, to be able to settle this conclusively, authors would have to do isotopic, histological and DNA work on living corals from their site, not just on skeletal material and MDAC. In addition, it would be worth noting that scleractinian corals are found embedded in ancient seep carbonates too (see Goedert and Peckmann 2005); there may be some useful comparative isotopic data in that paper.

**Response:** We included the paper by Goedert and Peckmann, 2005. We fully agree that analyses of coral tissues ( $\delta^{13}\text{C}$ , DNA) would add important information on their nutrition and metabolic relationships. However, we still regard  $\delta^{13}\text{C}$  values of their skeletons as valuable proxy for the possible uptake of  $\text{CH}_4$ . Corals utilize  $\text{HCO}_3^-$  deriving from both the environment and the internal production of  $\text{CO}_2$  for skeleton biomineralization (Swart, 1983; Zoccola et al., 2015; Nakamura et al., 2018). Therefore, if they uptake  $\text{CH}_4$  as a carbon source, the  $\text{CO}_2$  produced from  $\text{CH}_4$  metabolism would be used, and consequently parts of the  $\text{HCO}_3^-$  utilized for biomineralization would be isotopically depleted. This “mixing effect” would result in at least partially depleted  $\delta^{13}\text{C}$  values of the skeletons, similar to some chemosynthetic vesicomid and lucinid bivalves (Hein et al., 2006). The skeletons of the corals analyzed herein, however, exhibit significantly higher  $\delta^{13}\text{C}$  values than the co-occurring AOM-derived carbonates. Thus, they are not indicative for  $\text{CH}_4$  as important carbon source.

**20) Lines 364-367. The entombment of coral skeletons by MDAC may have no consequence to corals, if they are already dead. It's not entirely clear from the text if the corals associated with the MDAC are dead or alive. If they are alive then this argument is stronger. Also, in most seep environments MDACs form in the subsurface where AOM reactions are occurring. Is this the case at this site? What proof is there of active MDAC formation at the sediment-water interface, as indicated in Figure 12? This is pertinent to the arguments in section 4.3.**

**Response:** We cannot determine if the scleractinian corals embedded in AOM-derived carbonates (samples D10-R3 and D11-R8) were alive or dead when they were buried (lines 812-813 in the revised manuscript). However, we observed living corals in areas that are currently affected by seepage (e.g. the Northern Pompeia Coral Ridge, lines 262–263 in the revised manuscript; Fig. 6, C). Furthermore, we observed living octocorals growing on surfaces of currently formed AOM-derived carbonates (e.g., in an active pockmark in the Al Gacel MV, sample D10-R7; Fig. 5, C). These observations imply that corals in these regions are directly affected by methane seepage and the microbially mediated formation of carbonates due to AOM.

### **References**

Hein, J. R., Normark, W. R., McIntyre, B. R., Lorenson, T. D., and Powell, C. L.: Methanogenic calcite,  $^{13}\text{C}$ -depleted bivalve shells, and gas hydrate from a mud volcano offshore southern California, *Geology*, 34(2), 109–112, 2006.

- Nakamura, T., Nadaoka, K., Watanabe, A., Yamamoto, T., Miyajima, T., and Blanco, A. C.: Reef-scale modeling of coral calcification responses to ocean acidification and sea-level rise, *Coral Reefs*, 37, 2018.
- Swart, P. K.: Carbon and Oxygen Isotope Fractionation in Scleractinian Corals: a Review, *Earth-Sci. Rev.*, 19, 51–80, 1983.
- Zoccola, D., Ganot, P., Bertucci, A., Caminit-Segonds, N., Techer, N., Voolstra, C. R., Aranda, M., Tambutté, E., Allemand, D., Casey, J. R., and Tambutté, S.: Bicarbonate transporters in corals point towards a key step in the evolution of cnidarian calcification, *Sci. rep.-UK*, 5, 2015.

### **Authors response to Referee n° 3**

We are thankful for your useful and interesting comments. We hope we have addressed successfully the different issues discussed here.

#### ***Main issues***

-The authors write that the “This study aims at elucidating the linkage between the present-day formation of MDACs and CWCs development along the Pompeia Province (Fig. 1),”, but it is not clear why the selected analysis is the best way to achieve this. For example, “Petrographic analysis” is described in the Methods but it is not clear why this analysis is necessary to answer the questions addressed in the manuscript. The suspected nutritional linkage between CWC and hydrocarbon seepage is known in the literature as the ‘hydraulic theory’ (see Hovland, Jensen et al. 2012 and references therein). The present study is a direct test of this theory in an area that is very suited to test this. The name “hydraulic theory” and/or related reference are however not mentioned in the manuscript (e.g. ln 50-52)

**Response:** The “hydraulic theory” is now included in the introduction with references. Petrographic analyses are needed to be sure that these are seep carbonates, and to find the right sampling points for isotope analysis — we have to discriminate between authigenic carbonates, corals, micritic phases. of samples. For instance, embedded corals in some of the AOM-carbonates (D10-R3 and D11-R8) have been described and discriminated from the AOM-carbonate facies by petrographic analysis.

-Another major problem was description of the sampling design and the method of sampling. The authors write on line 84-86 “This study is based on collected data from the Pompeia Province, during the Subvent-2 cruise in 2014 aboard the R/V Sarmiento de Gamboa. The analysed samples were recovered from the Al Gacel MV (D10-R3, D10-R7, D11-R8) and the Northern Pompeia Coral Ridge (D03-B1) (Fig. 1).” This description is grossly inadequate. What was the sampling design? Are ‘samples’ collected ad random or based a preconceived plan? Why those sites? What material was sampled as ‘the samples’ (e.g. living coral pieces, coral rubble, sediment with rubble, carbonates)? Size/weight of the samples? Number of samples? Replication? How are the samples taken (ROV arm, push core)? How were samples stored on the ROV, how long before samples reached the surface how are samples processed/stored on-board (significant given the DNA/RNA analysis, e.g. with respect to cross contamination, microbial community shifts)?

**Detailed response to “What was the sampling design? Are ‘samples’ collected ad random or based a preconceived plan? Why those sites? How are the samples taken (ROV arm, push core)? How were samples stored on the ROV, how long before samples reached the surface how are samples processed/stored on-board (significant given the DNA/RNA analysis, e.g. with respect to cross contamination, microbial community shifts)?”:** we included more information on the study design, storage and sampling procedure in the material and methods section (see lines 89–100 on the new revised manuscript).

**Detailed response to “What material was sampled as ‘the samples’ (e.g. living coral pieces, coral rubble, sediment with rubble, carbonates)? Size/weight of the samples? Number of samples?”**

*Replication?*”: Information about the samples (what is each sample) is detailed in the “Petrography and stable isotopes of carbonates” results (section 3.3). Size of the samples are given with a scale bar in Fig. 7 (A, C, E, F). Weight of the samples was not determined. Each sample is one unit (i. e. coral fragment, carbonate from the based of the Al Gacel MV, carbonate from an active pockmark in Al Gacel MV, and carbonate from the summit of the Al Gacel MV). Replicates used for DNA analysis have been described in section 2.6.1. Furthermore, stable isotopic values obtained from precise sampling sites performed on each sample (section 2.4) are shown in Figure 7 (B, D, F) and Table 2.

**The authors are addressing ecological questions (see e.g. line 34-38, line 50-52 and line 75 “...present-day formation of MDACs and CWCs development...”) using studies of carbonates. One of the issues that is particularly relevant for the interpretation of these data is whether the analysis was performed on carbonates with living CWC or not. From the pictures and description, it seems plausible that only dead CWC carbonates were studied (although ln 348 mentions “the necrotic part of living *Madrepora*”), but this begs the question how representative the RNA/DNA/biomarker analysis is when only carbonates of dead CWCs are studied. To what extent do the authors think that the organic components of the carbonates still represent the CWC microbial community? Similarly for the <sup>13</sup>C carbonate analysis, is it known well enough whether CWCs leave a distinct isotope mark in the carbonates that is representative for feeding on surface derived organic matter versus hydrocarbons? Targeted sampling of also living CWC pieces and comparison with the sampled carbonates would have provided a means to address this.**

**Response:** since the necrotic coral-carbonate (D03-B1) used for environmental DNA analysis belongs to a living *Madrepora oculata* (see line 302), it is expected that 16S rDNA libraries reveal DNA related to microorganisms related to the corals’ microbiota. For instance, sequences related to Enterobacteria and Verrucomicrobia were found in this sample (Supplementary **Table S1**) and are normally in the environment and found associated with corals and other animals (Sorokin et al., 1995; Webster et al., 2016), while *Nitrosococcus* bacteria are ammonia-oxidizers, probably involved in the regulation of nitrogen cycle of the coral’s holobiont (Rädecker et al., 2015). Thus, we would have found DNA related to chemosynthetic microorganisms in case the coral fed from the seeping fluids.

Furthermore, it has been supported by many that coral-carbonate skeletons do partially reflect corals nutrition, since part of the HCO<sub>3</sub><sup>-</sup> used for its formation comes from the coral’s metabolism, i. e. CO<sub>2</sub> formed from cellular respiration (Swart, 1983; Zoccola et al., 2015; Nakamura et al., 2018) (lines 393–397 from the revised manuscript). Thus, stable carbon isotopic analysis is an optimal procedure to observe if corals used methane as a carbon source.

**-The authors mention that the ROV had sensors for CO<sub>2</sub> and CH<sub>4</sub> data and could take NISKIN water samples for CH<sub>4</sub>. In the results section (ln 219-221 and ln 231) CH<sub>4</sub> data are mentioned but in the M&M nothing can be found on sampling location (e.g. height above sediment), sensor calibration, samples handling, sample analyses of the water samples.**

**Response:** Pore-water analysis (from micro-cores) as well as seawater analysis (from Niskin bottles) have been included in this manuscript (see section 2.2.1). However, CH<sub>4</sub> measurements have not been included

in the material and methods section since those measurements have been done by colleagues from the Subevent-2 project which have previously published the methane values recovered from the Niskin bottles. Sampling procedure can be found in their publication (Sánchez-Guillamón et al., 2015).

**The site description in 3.1 should be partly moved to the Materials and Methods. Only the new results from this study should stay in 3.1.**

**Response:** the Pompeia Province region has been described in detail for the first time in this study. We provide geological structures in this area (Southern and Northern Pompeia Coral ridges, Cold-water Coral Mounds Fields), including novel data (e.g., bathymetry, seismics). Therefore, we consider it appropriate to report these findings in the results sections.

**-The authors infer that “severe seepage results in lethal conditions for CWCs” (line 363 - 364 and 377-378), but I see no evidence for that in the paper. In addition, the authors concluded that CWCs can be entombed by MDAC formation, it is however not clear whether this entombment is the cause of CWC mortality or that this entombment took place after CWC demise following for example from post-glacial decrease in current strength.**

**Response:** We cannot determine if the scleractinian corals embedded in AOM-derived carbonates (samples D10-R3 and D11-R8) were alive or dead when they were buried (lines 812–813 from revised manuscript). However, we observed living corals in areas that are currently affected by seepage (e.g. the Northern Pompeia Coral Ridge, lines 258–259 in the revised manuscript; Fig. 6, C). Furthermore, we observed living octocorals growing on surfaces of currently formed AOM-derived carbonates (e.g., in an active pockmark in the Al Gacel MV, sample D10-R7; Fig. 5, C). These observations indicate that CWCs can live when seepage occurs by means of the “buffer effect” (section 4.3) but severe seepage which cannot be completely buffered may end killing the CWCs.

*Suggestions for minor edits:*

**-ln 48-50: reduce number of refs**

**Response:** done.

**-ln 59: reduce number of refs**

**Response:** done.

**-ln 72-73: reduce number of refs**

**Response:** done.

**-ln 112: Please also give the values of the VPDB used, to avoid confusion**

**Response:** done. Please see lines 139–140 of the new revised manuscript.

**-ln 124: “have a global distribution” instead of “globally widespread”**

**Response:** done in line 16 of the revised manuscript.

**-In 152:** replace "... solid samples were..." with "...sample material was..."

**Response:** done.

**-In 230:** replace "...by dead.." with "... by shells of the chemosynthetic bivalves *Lucinoma*..."

**Response:** done.

**-In 243:** What does "virtually influenced" mean?

**Response:** "virtually" was deleted.

**-In 262:** "... values ranging from...". From the methods it is unclear on what this range is based, replication, multiple samples?

**Response:** The range is based on the different values obtained along the same petrographic facies of each sample (Figs. 7 & 9; Table 2). The numbers shown on the petrographic sections of each sample in Figure 7 (Fig. 7, B, D, F), indicate the exact sampling points used for stable isotopic analysis, which values are shown in Table 2. Further information has been included in the foot of Fig. 7 to facilitate this information for the readers.

**-In 307:** What does "proportions" here mean? Do you mean "rates" or "concentrations"?

**Response:** concentrations. Changed.

**-In 308:** So was methane sampled upon removal of the carbonate blocks?

**Response:** yes. Information added in line 347 of the new revised manuscript (see Sánchez-Guillamón et al., 2015 for details).

**-In 368:** The authors also mentioned the availability of a CO<sub>2</sub> sensor on the ROV. Has this been used to measure aragonite saturation states at the different locations?

**Response:** Because of the lack of exact data (x.c.f. Sánchez-Guillamón et al., 2015), aragonite saturation was not calculated. Interestingly, Niskin samples revealed high fCO<sub>2</sub> in Al Gacel MV above the seafloor (Sánchez-Guillamón et al., 2015), which may have an effect on the CWC, though experiments showed acclimation of *Lophelia* to changing aragonite saturation (Form et al., 2012). More accurate measurements would have been needed to approach the aragonite saturation state of the different locations.

**-In 755:** Fig 4C. There is a black pointing to "octocorals", but I cannot see these on the picture.

**Response:** they are on top of the carbonate, difficult to observed since they are semi-transparent. Figure was improved.

## **References**

- Form, A. U., and Riebesell, U.: Acclimation to ocean acidification during long-term CO<sub>2</sub> exposure in the cold-water coral *Lophelia pertusa*, *Global Change Biology*. 18, 843–853, 2012.
- Nakamura, T., Nadaoka, K., Watanabe, A., Yamamoto, T., Miyajima, T., and Blanco, A. C.: Reef-scale modeling of coral calcification responses to ocean acidification and sea-level rise, *Coral Reefs*, 37, 2018.
- Rädecker, N., Pogoreutz, C., Voolstra, C. R., Wiedenmann, J., and Wild, C: Nitrogen cycling in corals: The key to understanding holobiont functioning?, *Trends Microbiol.*, 23(8), 490–497, 2015.
- Sánchez-Guillamón, O., García, M. C., Moya-Ruiz, F., Vázquez, J. T., Palomino, D., Fernández-Puga, M. C., and Sierra, A.: A preliminary characterization of greenhouse gas (CH<sub>4</sub> and CO<sub>2</sub>) emissions from Gulf of Cádiz mud volcanoes, VIII Symposium MIA15, 2015.
- Sorokin, Y. I.: Coral reef ecology. Vol. 102, Springer Science & Business Media, 1995.
- Swart, P. K.: Carbon and Oxygen Isotope Fractionation in Scleractinian Corals: a Review, *Earth-Sci. Rev.*, 19, 51–80, 1983.
- Webster, N. S., Negri, A. P., Botté, E. S., Laffy, P. W., Flores, F., Noonan, S., ... and Uthicke, S.: Host-associated coral reef microbes respond to the cumulative pressures of ocean warming and ocean acidification, *Scientific reports*, 6, 19324, 2016.
- Zoccola, D. Ganot, P., Bertucci, A., Caminit-Segonds, N., Techer, N., Voolstra, C. R., Aranda, M., Tambutté, E., Allemand, D., Casey, J. R., and Tambutté, S.: Bicarbonate transporters in corals point towards a key step in the evolution of cnidarian calcification, *Sci. rep.-UK*, 5, 2015.

# 1 Cold-water corals and hydrocarbon-rich seepage in the 2 Pompeia Province (Gulf of Cádiz) — living on the edge

3 Blanca Rincón-Tomás<sup>1</sup>, Jan-Peter Duda<sup>2</sup>, Luis Somoza<sup>3</sup>, Francisco Javier González<sup>3</sup>, Dominik  
4 Schneider<sup>1</sup>, Teresa Medialdea<sup>3</sup>, Esther Santofimia<sup>4</sup>, Enrique López-Pamo<sup>4</sup>, Pedro Madureira<sup>5</sup>,  
5 Michael Hoppert<sup>1</sup>, and Joachim Reitner<sup>6,7</sup>

6 <sup>1</sup>Georg-August-University Göttingen, Institute of Microbiology and Genetics, Grisebachstraße 8, 37077  
7 Göttingen, Germany

8 <sup>2</sup>Department of Earth Sciences, University of California Riverside, CA 92521, USA

9 <sup>3</sup>Marine Geology Dept., Geological Survey of Spain, IGME, Ríos Rosas 23, 28003 Madrid, Spain

10 <sup>4</sup>Geological Resources Dept., Geological Survey of Spain, IGME, Ríos Rosas 23, 28003 Madrid, Spain

11 <sup>5</sup>Estrutura de Missão para a Extensão da Plataforma Continental (EMEPC). Rua Costa Pinto 165, 2770-047 Paço  
12 de Arcos, Portugal

13 <sup>6</sup>Georg-August-University Göttingen, Göttingen Centre of Geosciences, Goldschmidtstraße 3, 37077 Göttingen,  
14 <sup>7</sup>Germany<sup>3</sup>Göttingen Academy of Sciences and Humanities, Theaterstraße 7, 37073 Göttingen, Germany

15

16 *Correspondence to:* Blanca Rincón-Tomás (b.rincontomas@gmail.com)

17 **Abstract.** Azooxanthellate cold-water corals (CWCs) have a global distribution and have commonly been found  
18 in areas of active fluid seepage. The relationship between the CWCs and these fluids, however, is not well  
19 understood. This study aims at unraveling the relationship between CWC development and hydrocarbon-rich  
20 seepage in the Pompeia Province (Gulf of Cádiz, Atlantic Ocean). This region comprises mud volcanoes, coral  
21 ridges and fields of coral mounds, which are all affected by the tectonically driven seepage of hydrocarbon-rich  
22 fluids. The type of seepage such as focused, scattered, diffused or eruptive, is tightly controlled by a complex  
23 system of faults and diapirs. Early diagenetic carbonates from the currently active Al Gacel MV exhibit  $\delta^{13}\text{C}$ -  
24 signatures down to  $-28.77\text{‰}$  VPDB, indicating biologically derived methane as the main carbon source. The  
25 same samples contain  $^{13}\text{C}$ -depleted lipid biomarkers diagnostic for archaea such as crocetane ( $\delta^{13}\text{C}$  down to  $-101.2$   
26  $\text{‰}$  VPDB) and PMI ( $\delta^{13}\text{C}$  down to  $-102.9\text{‰}$  VPDB), evidencing microbially mediated anaerobic oxidation of  
27 methane (AOM). This is further supported by next generation DNA sequencing data, demonstrating the presence  
28 of AOM related microorganisms (ANME archaea, sulfate-reducing bacteria) in the carbonate. Embedded corals  
29 in some of the carbonates and CWC fragments exhibit less negative  $\delta^{13}\text{C}$  values ( $-8.08$  to  $-1.39\text{‰}$  VPDB),  
30 pointing against the use of methane as the carbon source. Likewise, the absence of DNA from methane- and  
31 sulfide-oxidizing microbes in a sampled coral does not support a chemosynthetic lifestyle of these organisms. In  
32 the light of these findings, it appears that the CWCs benefit rather indirectly from hydrocarbon-rich seepage by  
33 using methane-derived authigenic carbonates as a substratum for colonization. At the same time, chemosynthetic  
34 organisms at active sites prevent coral dissolution and necrosis by feeding on the seeping fluids (i. e. methane,  
35 sulfate, hydrogen sulfide), allowing cold-water corals to colonize carbonates currently affected by hydrocarbon-  
36 rich seepage.

## 37 1. Introduction

38 Cold-water corals (CWCs) are a widespread, non-phylogenetic group of cnidarians that include hard skeleton  
39 scleractinian corals, soft-tissue octocorals, gold corals, black corals and hydrocorals (Roberts et al., 2006; Roberts  
40 et al., 2009; Cordes et al., 2016). Typically, they thrive at low temperatures ( $4 - 12\text{°C}$ ) and occur in water depths

Con formato: Fuente: 10 pto

41 of ca. 50 – 4000 m. CWCs are azooxanthellate and solely rely on their nutrition as energy and carbon sources  
42 (Roberts et al., 2009). Some scleractinian corals (e.g. *Lophelia pertusa*, *Madrepora oculata*, *Dendrophyllia*  
43 *cornigera*, *Dendrophyllia alternata*, *Eguchipsammia cornucopia*) are able to form colonies or even large carbonate  
44 mounds (Rogers et al., 1999; Wienberg et al., 2009; Watling et al., 2011; Somoza et al., 2014). Large vertical  
45 mounds and elongated ridges formed by episodic growth of scleractinian corals (mainly *Lophelia pertusa*) are for  
46 instance widely distributed along the continental margins of the Atlantic Ocean (Roberts et al., 2009). These  
47 systems are of great ecological value since they offer sites for resting-, breeding-, and feeding for various  
48 invertebrates and fishes (Cordes et al., 2016 and references therein).

49 Several environmental forces influence the initial settling, growth, and decline of CWCs. These include, among  
50 others, an availability of suitable substrates for coral larvae settlement, low sedimentation rates, oceanographic  
51 boundary conditions (e.g. salinity, temperature and density of the ocean water) and a sufficient supply of nutrients  
52 through topographically controlled currents systems (Mortensen et al., 2001; Roberts et al., 2003; Thiem et al.,  
53 2006; Dorschel et al., 2007; Dullo et al., 2008; Van Rooij et al., 2011; Hebbeln et al., 2016). Alternatively, the  
54 “hydraulic theory” suggests that CWC ecosystems may be directly fueled by fluid seepage, providing a source of  
55 e.g. sulfur compounds, nitrogen compounds, P, CO<sub>2</sub> and/or hydrocarbons (Hovland, 1990; Hovland and Thomsen,  
56 1997; Hovland et al., 1998; 2012). This relationship is supported by the common co-occurrence of CWC-mounds  
57 and hydrocarbon-rich seeps around the world, for example at the Hikurangi Margin in New Zealand (Liebetrau et  
58 al., 2010), the Brazil margin (e.g. Gomes-Sumida et al., 2004), the Darwin Mounds in the northern Rockall Trough  
59 (Huvenne et al., 2009), the Kristin field on the Norwegian shelf (Hovland et al., 2012), the western Alborán Sea  
60 (Margreth et al., 2011), and the Gulf of Cádiz (e.g. Díaz-del-Río et al., 2003; Foubert et al., 2008). However,  
61 CWCs may also benefit rather indirectly from seepage. For instance, methane-derived authigenic carbonates  
62 (MDACs) formed through the microbially mediated anaerobic oxidation of methane (AOM; Suess & Whiticar,  
63 1989; Hinrichs et al., 1999; Thiel et al., 1999; Boetius et al., 2000; Hinrichs & Boetius, 2002) potentially provide  
64 hard substrata for larval settlement (e.g. Díaz-del-Río et al., 2003; Van Rooij et al., 2011; Magalhães et al. 2012;  
65 Le Bris et al., 2016; Rueda et al., 2016). In addition, larger hydrocarbon-rich seepage related structures such as  
66 mud volcanoes and carbonate mud mounds act as morphological barriers favoring turbulent water currents that  
67 deliver nutrients to the corals (Roberts et al., 2009; Wienberg et al., 2009; Margreth et al., 2011; Vandorpe et al.,  
68 2016).

69 In the Gulf of Cádiz, most CWC occurrences are “coral graveyards” with only a few living corals that are situated  
70 along the Iberian and Moroccan margins. These CWC systems are typically associated with diapiric ridges, steep  
71 fault-controlled escarpments, and mud volcanoes (MVs) such as the Faro MV, Hesperides MV, Mekness MV, and  
72 mud volcanoes in the Pen Duick Mud Volcano Province (Foubert et al., 2008; Wienberg et al., 2009). Mud  
73 volcanoes (and other conspicuous morphological structures in this region such as pockmarks) are formed through  
74 tectonically induced fluid flow (Pinheiro et al., 2003; Somoza et al., 2003; Medialdea et al., 2009; León et al.,  
75 2010; 2012). The fluid flow is promoted through the of the high regional tectonic activity and high fluid contents  
76 of sediments in this area (mainly CH<sub>4</sub> and, to a lesser extent, H<sub>2</sub>S, CO<sub>2</sub>, and N<sub>2</sub>; Pinheiro et al., 2003; Hensen et  
77 al., 2007; Scholz et al., 2009; Smith et al., 2010; González et al., 2012). However, the exact influence of fluid flow  
78 on CWC growth in this region remains elusive.

79 This study aims at elucidating the linkage between the present-day formation of MDACs and CWCs development,  
80 by testing whether CWCs are indeed non-chemosynthetic fauna or harbor in fact chemosynthetic symbionts which  
81 allow them consuming some of the reduced compounds in sites of active emission of under seafloor fluids. We

82 address our hypothesis by the combined analyses of high-resolution ROV underwater images, geophysical data  
83 (e.g. seabed topography, deep high-resolution multichannel seismic reflection data), and sample materials (water  
84 analysis, petrographic features,  $\delta^{13}\text{C}$ - and  $\delta^{18}\text{O}$ -signatures of carbonates, lipid biomarkers and environmental  
85 rDNA sequences of the prokaryotic microbial community). We focus our study in the Pompeia Province (**Fig. 1**),  
86 which encompasses mud volcanoes as the currently active Al Gacel MV (León et al., 2012), diapiric coral ridges  
87 and mounds. Based on our findings, we propose an integrated model to explain the tempo-spatial and genetic  
88 relations between CWCs, chemosynthetic fauna and hydrocarbon-rich seepage in the study area.

## 89 2. Materials and Methods

90 This study is based on data and samples from the Pompeia Province that were collected during the Subvent-2  
91 cruise in 2014 aboard the R/V Sarmiento de Gamboa (**Fig. 1**). In order to elucidate the tempo-spatial and genetic  
92 relations between CWCs, chemosynthetic fauna and hydrocarbon-rich seepage in this area, we explored geological  
93 features (mud volcanoes and coral ridges) by means of underwater imaging and geophysical data. ROV dives were  
94 carried out at the Al Gacel MV (D10 and D11) and the Northern Pompeia Coral Ridge (D03). Subsequently, we  
95 conducted detailed analyses on selected samples from sites that were characterized by different types of seepage  
96 during sampling (**Table 1**). Samples from the Al Gacel MV include authigenic carbonates (D10-R3, D10-R7, D11-  
97 R8), pore-water from the sediment (via micro-cores; D10-C5, D10-C8, D11-C10), and water from above the  
98 seafloor (via Niskin bottles; D10-N12, D11-N9). Furthermore, a scleractinian coral fragment was recovered from  
99 the Northern Pompeia Coral Ridge (D03-B1). All samples were immediately stored at room temperature  
100 (petrographic analysis), 4 °C (water, sediments and pore-water analysis), -20 °C (stable isotopic analysis), or -80  
101 °C (environmental DNA analysis).

### 102 2.1. Geophysical survey

103 Seabed topography of the studied sites was mapped by using an Atlas Hydrosweep DS (15 kHz and 320 beams)  
104 multibeam echosounder (MBES). Simultaneously, ultra-high resolution sub-bottom profiles were acquired with  
105 an Atlas Parasound P-35 parametric chirp profiler (0.5 – 6 kHz). Deep high-resolution multichannel seismic  
106 reflection data was obtained using an array of 7 SERCEL gi-guns (system composed of 250 + 150 + 110 + 45  
107 cubic inches) with a total of 860 cubic inches. The obtained data were recorded with an active streamer  
108 (SIG@16.3x40.175; 150 m length with 3 sections of 40 hydrophones each). The shot interval was 6 seconds and  
109 the recording length 5 seconds two-way travel time (TWT). Data processing (filtering and stacking) was performed  
110 on board with Hot Shots software.

### 111 2.2. Video survey and analysis

112 A remotely operated vehicle (ROV-6000 Luso, operated by EMEPC) was used for photographic documentation  
113 (high definition digital camera, 1024x1024 pixel) and sampling. The ROV was further equipped with a STD/CTD-  
114 SD204 sensor (*in-situ* measurements of salinity, temperature, oxygen, conductivity, sound velocity and depth),  
115 HydroC<sup>TM</sup> sensors (*in-situ* measurements of CO<sub>2</sub> and CH<sub>4</sub>), Niskin bottles (CH<sub>4</sub> concentrations, pH and redox  
116 potential measurements), and a ROV core sampler (up to 16 cm).

#### 117 2.2.1. Seawater and pore-water analysis

118 Niskin water-samples and micro-cores covering the water/sediment interface were recovered from an active  
119 pockmark close to the summit of the Al Gacel MV (D10-N4, D10-C5, D10-C8; same site as carbonate-sample  
120 D10-R7) as well as directly from its summit (D11-N9, D11-C10). Redox potentials (ORP) and pH-values of the  
121 water contained in the Niskin bottles were measured on site with HANNA portable instruments (HI 9025). Pore-  
122 water from the micro-cores was immediately extracted by centrifuging 10 cm thick slices of the sediments. Upon  
123 extraction, the pore-water was filtered with syringe filters of cellulose acetate (0.2  $\mu\text{m}$  pore), acidified with distilled  
124 nitric acid ( $\text{HNO}_3$ ), and stored under 4 °C before further analysis. Major and trace elements were subsequently  
125 measured with an Agilent 7500c inductively coupled plasma mass spectrometer (ICP-MS). Method accuracy and  
126 precision was checked by external standards (MIV, EPA, NASC, CASS). The precision was better than 5 % RSD  
127 (residual standard deviation) and the accuracy better than 4%. Concentrations of  $\text{S}^{2-}$  were measured with a Hanch-  
128 Lange DR 2800 spectrophotometer (cuvette test kit LCK 653).

### 129 **2.3. Petrographic analysis**

130 General petrographic analysis was performed on thin sections (ca. 60  $\mu\text{m}$  thickness) with a Zeiss SteREO  
131 Discovery.V8 stereomicroscope (transmitted- and reflected light) linked to an AxioCam MRc 5-megapixel camera.  
132 Additional detailed petrographic analysis of textural and mineralogical features was conducted on polished thin  
133 sections (ca. 30  $\mu\text{m}$  thickness) using a DM2700P Leica Microscope coupled to a DFC550 digital camera.  
134 Carbonate textures have been classified following Dunham (1962) and Embry & Klovan (1971).

### 135 **2.4. Stable isotope signatures ( $\delta^{13}\text{C}$ , $\delta^{18}\text{O}$ ) of carbonates**

136 Stable carbon and oxygen isotope measurements were conducted on ca. 0.7 mg carbonate powder obtained with a  
137 high precision drill ( $\varnothing$  0.8 mm). The analyses were performed with a Thermo Scientific Kiel IV carbonate device  
138 coupled to a Finnigan Delta Plus gas isotope mass spectrometer. Accuracy and reproducibility were checked  
139 through the replicate analysis of a standard (NBS19) and reproducibility was better than 0.1 ‰. Stable carbon and  
140 oxygen isotope values are expressed in the standard  $\delta$  notation as per mill (‰) deviations relative to Vienna Pee  
141 Dee Belemnite (VPDB).

### 142 **2.5. Lipid biomarker analysis**

#### 143 **2.5.1. Sample preparation**

144 All materials used were pre-combusted (500 °C for >3 h) and/or extensively rinsed with acetone prior to sample  
145 contact. A laboratory blank (pre-combusted sea sand) was prepared and analyzed in parallel to monitor laboratory  
146 contaminations.

147 The preparation and extraction of lipid biomarkers was conducted in orientation to descriptions in Birgel et al.  
148 (2006). Briefly, the samples were first carefully crushed with a hammer and internal parts were powdered with a  
149 pebble mill (Retsch MM 301, Haan, Germany). Hydrochloric acid (HCl; 10 %) was slowly poured on the powdered  
150 samples which were covered with dichloromethane (DCM)-cleaned water. After 24 h of reaction, the residues (pH  
151 3 – 5) were repeatedly washed with water and then lyophilized.

152 3 g of each residue was saponified with potassium hydroxide (KOH; 6 %) in methanol (MeOH). The residues were  
153 then extracted with methanol (40 mL, 2x) and, upon treatment with HCl (10 %) to pH 1, in DCM (40 mL, 2x) by  
154 using ultra-sonification. The combined supernatants were partitioned in DCM vs. water (3x). The total organic

155 extracts (TOEs) were dried with sodium sulfate (NaSO<sub>4</sub>) and evaporated with a gentle stream of N<sub>2</sub> to reduce loss  
156 of low-boiling compounds (cf. Ahmed and George, 2004).  
157 Fifty percent of each TOE was separated over a silica gel column (0.7 g Merck silica gel 60 conditioned with *n*-  
158 hexane; 1.5 cm i.d., 8 cm length) into (a) hydrocarbon (6 mL *n*-hexane), (b) alcohol (7 mL DCM/acetone, 9:1, v:v)  
159 and (c) carboxylic acid fractions (DCM/MeOH, 3:1, v:v). Only the hydrocarbons were subjected to gas  
160 chromatography–mass spectrometry (GC-MS).

### 161 2.5.2. Gas chromatography–mass spectrometry (GC-MS)

162 Lipid biomarker analyses of the hydrocarbon fraction were performed with a Thermo Scientific Trace 1310 GC  
163 coupled to a Thermo Scientific Quantum XLS Ultra MS. The GC was equipped with a capillary column  
164 (Phenomenex Zebron ZB-5MS, 30 m length, 250 μm inner diameter, 0.25 μm film thickness). Fractions were  
165 injected into a splitless injector and transferred to the column at 300 °C. The carrier gas was He at a flow rate of  
166 1.5 mL min<sup>-1</sup>. The GC oven temperature was ramped from 80°C (1 min) to 310 °C at 5 °C min<sup>-1</sup> (held for 20 min).  
167 Electron ionization mass spectra were recorded in full scan mode at an electron energy of 70 eV with a mass range  
168 of *m/z* 50 – 600 and scan time of 0.42 s. Identification of individual compounds was based on comparison of mass  
169 spectra and GC retention times with published data and reference compounds.

### 170 2.5.3 Gas chromatography–combustion–isotope ratio mass spectrometer (GC-C-IRMS)

171 Compound specific δ<sup>13</sup>C analyses were conducted with a Trace GC coupled to a Delta Plus IRMS via a  
172 combustion-interface (all Thermo Scientific). The combustion reactor contained CuO, Ni and Pt and was operated  
173 at 940°C. The GC was equipped with two serially linked capillary columns (Agilent DB-5 and DB-1; each 30 m  
174 length, 250 μm inner diameter, 0.25 μm film thickness). Fractions were injected into a splitless injector and  
175 transferred to the GC column at 290°C. The carrier gas was He at a flow rate of 1.2 ml min<sup>-1</sup>. The temperature  
176 program was identical to the one used for GC-MS (see above). CO<sub>2</sub> with known δ<sup>13</sup>C value and a standard  
177 (IAEA600) were used for internal calibration. Instrument precision was checked using a mixture of *n*-alkanes with  
178 known isotopic composition. Standard deviations of duplicate sample measurements were generally better than  
179 1.0 ‰. Carbon isotope ratios are expressed as δ<sup>13</sup>C (‰) relative to VPDB.

## 180 2.6. Amplicon sequencing of 16S rRNA genes

### 181 2.6.1. DNA extraction and 16S rRNA gene amplification

182 Environmental DNA analyses of microbial communities were performed on a carbonate sample with embedded  
183 corals from the base of the Al Gacel MV (D10-R3), a carbonate sample from an active pockmark close to the  
184 summit of the Al Gacel MV (D10-R7), and a necrotic fragment of a living *Madrepora oculata* recovered from the  
185 Northern Pompeia Coral Ridge (D03-B1). About 1 – 4 g of solid samples were first mashed with mortar and liquid  
186 nitrogen to fine powder. Three biological replicates were used per sample. Total DNA was isolated with a Power  
187 Soil DNA Extraction Kit (MO BIO Laboratories, Carlsbad, CA). All steps were performed according to the  
188 manufacturer's instructions.

189 Bacterial amplicons of the V3 – V4 region were generated with the primer set MiSeq\_Bacteria\_V3\_forward  
190 primer (5'-TCGTCGGCAGCGTCAGATGTGTATAAGAGACAGCCTACGGGNGGCWGCAG-3') and  
191 MiSeq\_Bacteria\_V4\_reverse primer (5'-

Con formato: Fuente: 10 pto

192 GTCTCGTGGGCTCGGAGATGTGTATAAGAGACAGGACTACHVGGGTATCTAATCC-3'). Likewise,  
193 archaeal amplicons of the V3 – V4 region were generated with the primer set MiSeq\_Archaea\_V3\_forward primer  
194 (5'-TCGTCGGCAGCGTCAGATGTGTATAAGAGACAG-GGTGBCAGCCGCGCGTAA-3') and  
195 MiSeq\_Archaea\_V4\_reverse primer (5'-GTCTCGTGGGCTCGGAGATGTGTATAAGAGACAG-  
196 CCCGCCAATTYCTTTAAG-3'). 50 µl of the PCR reaction mixture for bacterial DNA amplification, contained  
197 1 U Phusion high fidelity DNA polymerase (Biozym Scientific, Oldendorf, Germany), 5% DMSO, 0.2 mM of  
198 each primer, 200 µM dNTP, 0.15 µl of 25 mM MgCl<sub>2</sub>, and 25 ng of isolated DNA. The PCR protocol for bacterial  
199 DNA amplification included (i) initial denaturation for 1 min at 98 °C, (ii) 25 cycles of 45 s at 98 °C, 45 s at 60 °C,  
200 and 30 s at 72 °C, and (iii) a final extension at 72 °C for 5 min. The PCR reaction mixture for archaeal DNA  
201 amplification was similarly prepared but contained instead 1 µl of 25 mM MgCl<sub>2</sub> and 50 ng of isolated DNA. The  
202 PCR protocol for archaeal DNA amplification included (i) initial denaturation for 1 min at 98 °C, (ii) 10 cycles of  
203 45 s at 98 °C, 45 s at 63 °C, and 30 s at 72 °C, (iii) 15 cycles of 45 s at 98 °C, 45 s at 53 °C, and 30 s at 72 °C, and  
204 (iv) a final extension at 72 °C for 5 min.  
205 PCR products were checked by agarose gel electrophoresis and purified using the GeneRead Size Selection Kit  
206 (QIAGEN GmbH, Hilden, Germany).

## 207 2.6.2. Data analysis and pipeline

208 Illumina PE sequencing of the amplicons and further process of the sequence data were performed in the Göttingen  
209 Genomics Laboratory (Göttingen, Germany). After Illumina MiSeq processing, sequences were analyzed as  
210 described in Egelkamp et al. (2017) with minor modifications. In brief, paired-end sequences were merged using  
211 PEAR v0.9.10 (Zhang et al., 2014), sequences with an average quality score below 20 and containing unresolved  
212 bases were removed with QIIME 1.9.1 (Caporaso et al., 2010). Non-clipped reverse and forward primer sequences  
213 were removed by employing cutadapt 1.15 (Martin, 2011). USEARCH version 9.2.64 was used following the  
214 UNOISE pipeline (Edgar, 2010). In detail, reads shorter than 380 bp were removed, dereplicated, and denoised  
215 with the UNOISE2 algorithm of USEARCH resulting in amplicon sequence variants (ASVs) (Callahan et al.,  
216 2017). Additionally, chimeric sequences were removed using UCHIME2 in reference mode against the SILVA  
217 SSU database release 132 (Yilmaz et al., 2014). Merged paired-end reads were mapped to chimera-free ASVs and  
218 an abundance table was created using USEARCH. Taxonomic classification of ASVs was performed with BLAST  
219 against the SILVA database 132. Extrinsic domain ASVs, chloroplasts, and unclassified ASVs were removed from  
220 the dataset. Sample comparisons were performed at same surveying effort, utilizing the lowest number of  
221 sequences by random subsampling (20,290 reads for bacteria, 13,900 reads for archaea).  
222 The paired-end reads of the 16S rRNA gene sequencing were deposited in the National Center for Biotechnology  
223 Information (NCBI) in the Sequence Read Archive SRP156750.

## 224 3. Results

### 225 3.1. The Pompeia Province — geological settings

226 The Pompeia Province is situated in the Gulf of Cádiz offshore Morocco, within the so-called Middle Moroccan  
227 Field (Ivanov et al., 2000) at water-depths between 860 and 1000 m (Fig. 1). It encompasses the active Al Gacel  
228 MV (Fig. 1, C), another mud volcano which is extinct (further referred as extinct MV) and two east-west elongated  
229 ridges (Northern Pompeia Coral Ridge and Southern Pompeia Coral Ridge). CWCs occur on all of these

230 morphological features and scattered coral-mounds surround the ridges with a smooth relief (Fig. 1, B). Detailed  
231 geological profiles and 3D images of these features are shown in Figs. 2 and 3.

232 The Al Gacel MV is a cone-shape structure, 107 m high and 944 m wide, with its summit at 762 m depth and  
233 surrounded by a 11 m deep rimmed depression (León et al., 2012) (Fig. 1, C). It is directly adjacent to the Northern  
234 Pompeia Coral Ridge (Fig. 2, A–B), which extends ca. 4 km in westward direction (Fig. 2, A–B) and it is  
235 terminated by the Pompeia Escarpment (Fig. 1, B; Fig. 2, C). High resolution seismic profiles of the Pompeia  
236 Escarpment show CWC build-ups (R1 to R4) with steep lateral scarps of ca. 40 m height (Fig. 2, C). The Al Gacel  
237 MV is of sub-circular shape and exhibits a crater at its top (Fig. 2, A–B).

238 Ultra-high resolution sub-bottom seismic profile crossing the Pompeia Province from northwest (NW) to southeast  
239 (SE) (Fig. 3, A), shows (i) the Al Gacel MV surrounded by bottom-current deposits, (ii) an up to 130 m high CWC  
240 framework, growing on top the Southern Pompeia Coral Ridge, and (iii) semi-buried CWC mounds surrounding  
241 the ridge in areas of low relief. These CWC mounds locally form smooth, up to 25 – 30 m high topographic reliefs  
242 that are exposed, but then taper downward below the seafloor (applying sound speeds of 1750 m/s in recent  
243 sediments). Additionally, a multichannel seismic profile following the same track but with higher penetration  
244 below the seafloor (Fig. 3, B) shows high amplitude reflections inside the Al Gacel cone and enhanced reflections  
245 at the top of the diapirs (yellow dotted-line in Fig. 3, B), pointing to the occurrence of gas (hydrocarbon)-charged  
246 sediments. It furthermore exhibits breaks in seismic continuity and diapiric structures at different depths below the  
247 Southern Pompeia Coral Ridge and the Al Gacel MV, evidencing the presence of a fault system (Fig. 3, B). These  
248 tectonic structures may promote the development of overpressure areas (OP in Fig. 3, B) and consequent upward  
249 fluid flow to the surface.

### 250 3.2. ROV observation and measurements

251 Submersible ROV surveys at the Al Gacel MV (Fig. 1, C) revealed the presence of dispersed pockmark  
252 depressions at the eastern (Dive 10, 790 m) and northern flanks (Dive 11, 760 – 825 m depth). These sites are  
253 characterized by focused but low intensity seafloor bubbling (e.g. Fig. 4, B; Fig. 5, A). Analysis of water samples  
254 revealed CH<sub>4</sub>-concentration up to 171 nM during Dive 10 and up to 192 nM during Dive 11 (Sánchez-Guillamón  
255 et al., 2015).

256 Pockmarks are typically characterized by grey-olive mud breccia sediments and authigenic carbonates, appearing  
257 in the center and edges. The authigenic carbonates are commonly associated with typical methane-seep related  
258 organisms (e.g. sulfide-oxidizing bacterial mats, chemosynthetic bivalves, siboglinid tubeworms) (Fig. 4, B–C;  
259 Fig. 5). Communities of non-chemosynthetic organisms (e.g. sponges, corals) were also found at pockmarks (Fig.  
260 4, B–C; Fig. 5, C), but were more abundant in places where no seepage was detected (Fig. 4, A).

261 Observations with the submersible ROV at the Northern Pompeia Coral Ridge and the extinct MV (Dive 03)  
262 revealed widespread and abundant occurrences of dead scleractinian-corals (mainly *Madrepora oculata* and  
263 *Lophelia pertusa*) currently colonized by few living non-chemosynthetic organisms (e.g. *Corallium tricolor*, other  
264 octocorals, sea urchins) (Fig. 6, B–D). Locally, grey-black colored patches of sulfide-oxidizing bacterial mats  
265 surrounded by dead chemosynthetic bivalves (*Lucinoma asapeus* and *Thysira vulcolutre*) were observed (Fig. 6,  
266 A). CH<sub>4</sub>-seepage appeared to be less than at the Al Gacel MV, with concentrations of 80 – 83 nM.

267 Water parameters display homogenous values between the four sampling sites (10 °C temperature, ca. 52 – 55 %  
268 dissolved oxygen, ca. 31 Kg/m<sup>3</sup> density) (Table 2). At depths of 790 m (D10-N4, same site as carbonate D10-R7)  
269 and 760 m (D11-N9), the pH of seawater was 7.88 and 7.85, respectively (Table 3). The same seawater samples

270 exhibited ORP values of 136 mV (D10-N4) and 257 mV (D11-N9) (Table 3). Further analysis of these seawater  
271 samples revealed Fe<sup>2+</sup> concentration of 0.57 and 0.31 μM, while S<sup>2-</sup> values were nearly absent (below detection  
272 limit) (Table 2). Fe<sup>2+</sup> concentrations in pore-waters ranged between 0.94 – 1.27 μM (D10-C5), 2.70 – 1.74 μM  
273 (D10-C8), and 2.39 – 5.32 μM (D11-C10). S<sup>2-</sup> concentrations in pore-waters were below detection limit (D10-C5),  
274 50.23 μM (D10-C8), and 0.47 μM (D11-C10) (Table 3).

### 275 3.3. Petrography and stable isotopes signatures of carbonates (δ<sup>18</sup>O, δ<sup>13</sup>C)

276 Sample D10-R3 derives from a field of carbonates at the base of the Al Gacel MV which is inhabited by sponges  
277 and corals (Fig. 4, A). The sample is a frammestone composed of deep water scleractinian corals (*Madrepora* and  
278 rare *Lophelia*) (Fig. 7, A–B). The corals are typically cemented by microbial automicrite (*sensu* Reitner et al.  
279 1995) followed by multiple generations of aragonite. A matrix of dark allomicrite (*sensu* Reitner et al. 1995) with  
280 oxidized framboidal pyrites and remains of planktonic foraminifera is restricted to few bioerosional cavities (ca.  
281 5%) in the skeletons of dead corals (Fig. 8, A–B). δ<sup>13</sup>C signatures of the matrix and cements range from –26.68 to  
282 –18.38 ‰, while the embedded coral fragments exhibit δ<sup>13</sup>C values between –5.58 and –2.09 ‰ (Fig. 7, B; Table  
283 4). The δ<sup>18</sup>O values generally range from +2.35 to +3.92 ‰ (Fig. 9; Table 4).

284 Sample D10-R7 was recovered from a pockmark on the eastern site of the Al Gacel MV that is virtually influenced  
285 by active seepage (Fig. 3, C). It consists of black carbonate and exhibits a strong hydrogen sulfide (H<sub>2</sub>S) odor (Fig.  
286 5, B; Fig. 7, C–D). The top of this sample was inhabited by living octocorals (Fig. 5, C), while chemosymbiotic  
287 siboglinid worms were present on the lower surface (Fig. 5, D). The sample is characterized by a grey peloidal  
288 wackestone texture consisting of allomicrite with abundant planktonic foraminifers and few deep water miliolids.  
289 The sample furthermore exhibits some fractured areas which are partly filled by granular and small fibrous cement,  
290 probably consisting of Mg-calcite. Locally, light brownish crusts of microbial automicrite similar to ones in D10-  
291 R3 are present (see above). Framboidal pyrite is abundant and often arranged in aggregates (Fig. 8, C–D). The  
292 carbonate exhibits δ<sup>13</sup>C values ranging from –28.77 to –21.13 ‰ and δ<sup>18</sup>O values from +2.37 to +3.15 ‰ (Fig. 9;  
293 Table 4).

294 Sample D11-R8 comes from an area with meter-sized carbonate blocks at the summit of the Al Gacel MV and is  
295 mainly colonized by sponges and serpulid worms (Fig. 4, D). The sample generally exhibits a light grey mud- to  
296 wackestone texture consisting of allomicrite with few scleractinian-coral fragments and planktonic foraminifers  
297 (Fig. 7, E–F). The carbonate furthermore contains abundant quartz silt and, locally, pyrite enrichments. A further  
298 prominent feature are voids that are encircled by dark grey halos and exhibit brownish margins (due to enrichments  
299 of very small pyrite crystals and organic matter, respectively). δ<sup>13</sup>C signatures of the matrix and cements range  
300 from –14.82 to –14.74 ‰, while embedded coral fragments exhibit δ<sup>13</sup>C values of –4.91 to –2.99 ‰ (Fig. 7, F;  
301 Table 4). δ<sup>18</sup>O values generally range from +1.49 to +5.60 ‰ (Fig. 9; Table 4).

302 Sample D03-B1 is a necrotic fragment of a living scleractinian coral (*Madrepora oculata*) recovered from the  
303 Northern Pompeia Coral Ridge (Fig. 6, D; Fig. 7, G). The coral-carbonate exhibits δ<sup>13</sup>C values ranging from –8.08  
304 to –1.39 ‰ and δ<sup>18</sup>O values from –0.31 to +2.26 ‰ (Fig. 9; Table 4).

### 305 3.4. Lipid biomarkers and compound specific carbon isotope signatures

306 The hydrocarbon fractions of the carbonate recovered from the active pockmark (D10-R7) mainly consist of the  
307 irregular, tail-to-tail linked acyclic isoprenoids 2,6,11,15-tetramethylhexadecane (C<sub>20</sub>; crocetane), 2,6,10,15,19-

308 pentamethylcosane (C<sub>25</sub>; PMI), as well as of several unsaturated homologues of these compounds (Fig. 10).  
309 Additionally, it contains the regular, head-to-tail linked acyclic isoprenoid pristane (C<sub>19</sub>).  
310 The hydrocarbon fraction of the carbonate recovered from the summit of the Al Gacel MV (D11-R8) is dominated  
311 by *n*-alkanes with chain-lengths ranging from C<sub>14</sub> to C<sub>33</sub> (maxima at *n*-C<sub>16</sub> and, subordinated, at *n*-C<sub>20</sub> and *n*-C<sub>31</sub>)  
312 (Fig. 10). The sample further contains pristane, a mixture of crocetane and the head-to-tail linked acyclic  
313 isoprenoid phytane (C<sub>20</sub>) (co-eluting), as well as traces of PMI.  
314 In the carbonate from the active pockmark (D10-R7), crocetane and PMI exhibited strongly depleted δ<sup>13</sup>C values  
315 (−101.2 ‰ and −102.9 ‰, respectively). In the carbonate from the summit of the volcano (D11-R8),  
316 crocetane/phytane and PMI showed less depleted δ<sup>13</sup>C values (−57.2 ‰ and −74.3 ‰, respectively). δ<sup>13</sup>C values  
317 of *n*-alkanes in the carbonate D11-R8 (*n*-C<sub>17-22</sub>) ranged between −30.8 ‰ and −33.0 ‰ (Table 5).

### 318 3.5. DNA inventories (MiSeq Illumina sequences)

319 Bacterial DNA from samples D10-R3 (authigenic carbonate, base of the Al Gacel MV) and D03-B1 (*Madrepora*  
320 *oculata* fragment, Northern Pompeia Coral Ridge) mainly derives from taxa that typically thrive in the water-  
321 column (e. g. Actinobacteria, Acidobacteria, Chloroflexi, Bacteroidetes, Woeseiaceae, Dadabacteria,  
322 Kaiserbacteria, Poribacteria, Planctomycetes, Gemmatimonadetes) (Fig. 11, A). The sample D10-R3 furthermore  
323 contains bacterial DNA of the nitrite-oxidizing bacteria *Nitrospira sp.*, while the sample D03-B1 contains DNA  
324 of the bacterial taxa Verrucomicrobia, Enterobacteria, and *Nitrosococcus*. Noteworthy, one amplicon sequence  
325 variant (ASV\_189) with low number of clustered sequences has been found in D03-B1, identified as a  
326 methanotrophic symbiont of *Bathymodiolus mauritanicus* (see Rodrigues et al., 2013).  
327 Up to 50 % of bacterial DNA in sample D10-R7 (authigenic carbonate, top of the Al Gacel MV) derives from taxa  
328 that are commonly associated with fluid seepage and AOM, i.e. sulfide-oxidizing bacteria, sulfate-reducing  
329 bacteria (SRB) and methane-oxidizing bacteria. The most abundant are SRB taxa like SEEP-SRB1, SEEP-SRB2,  
330 *Desulfatiglans*, *Desulfobulbus* and *Desulfococcus*, which typically form consortia with ANME archaea.  
331 Archaeal DNA (Fig. 11, B) from samples D10-R3 and D03-B1 mainly consist of *Cenarchaeum sp.*, which  
332 represents 70 – 90 %. *Candidatus Nitrosopumilus* is the second most abundant in both samples, representing 5 –  
333 20 %. In contrast, around 90 % of archaeal DNA in D10-R7 is related to ANME-1 and ANME-2 groups, in good  
334 concordance with the relative abundances of SRB DNA.  
335 Details of the number of reads per taxa are shown in the supplementary data, Tables 1 and 2.

## 336 4. Discussion

### 337 4.1. Evidence for hydrocarbon-rich seepage affecting the Pompeia Province

338 Two-dimensional multichannel-seismic images show that the Pompeia Province is affected by fluid expulsion  
339 related to compressional diapiric ridges and thrust faults (Fig. 3, B), as it has been reported from other areas of the  
340 Gulf of Cádiz (Somoza et al., 2003; Van Rensbergen et al., 2005; Medialdea et al., 2009). There seem to be  
341 different types of fault-conduit systems that link the overpressure zones (OP) with the seafloor (Fig. 3, B),  
342 controlling both the type and rate of seepage (e.g. eruptive, focused, diffused or intermittent, the latter referred to  
343 as “dripping-like” in the following). At the Al Gacel MV, conduits are for instance mainly linked to faults and a  
344 dense hydro-fracture network, allowing the migration of hydrocarbon-rich muds from the overpressure zone to the  
345 surface. During active episodes, eruptions lead to the formation of mud-breccia flows as observed in gravity cores

346 (e.g. León et al., 2012). During rather dormant episodes, focused and dripping-like seepage predominates, forming  
347 pockmark features (**Fig. 4, B**).

348 Currently, the Al Gacel MV is affected by continuous and focused dripping-like seepages. These sites of active  
349 seepage are characterized by carbonates that are suspected to be methane-derived (e.g. sample D10-R7, **Fig. 4, B–**  
350 **C**). In-situ ROV-measurements and subsequent water sample analysis demonstrated high concentrations of CH<sub>4</sub>  
351 in fluids that were escaping upon removal of the carbonate D10-R7 from the active pockmark (171 nM; **Fig. 5, A**)  
352 (Sánchez-Guillamón et al., 2015). This association suggests a genetic relationship between hydrocarbon-rich  
353 seepage and the carbonate, as also reflected low δ<sup>13</sup>C-signatures of the carbonates analyzed herein (down to ca.  
354 –30 ‰, **Fig. 9; Table 3**). Indeed, the grey peloidal texture of this sample resembles that of AOM-derived  
355 automicrites from the Black Sea that are related to micro-seepage of methane (cf. Reitner et al., 2005). The here  
356 observed isotopically depleted acyclic isoprenoids such as crocetane and PMI (δ<sup>13</sup>C values between ca. –103 and  
357 –57‰; **Fig. 10; Table 4**) are typical fingerprints of AOM-associated Archaea (Hinrichs et al., 1999; Thiel et al.,  
358 1999, 2001; Peckmann et al., 2001; Peckmann & Thiel, 2004), which is also in good accordance with the high  
359 abundance of DNA related to ANME. At the same time, elevated concentrations of S<sup>2-</sup> and Fe<sup>2+</sup> in pore-waters of  
360 D10-C8 micro-core (0.23 μM and 1.74 μM, respectively; **Table 2**), abundant framboidal pyrite (**Fig. 8, C–D**) and  
361 SRB-related DNA in the carbonate (**Fig. 11**) evidence microbial sulfate reduction in the environment. All these  
362 data clearly demonstrate that the carbonates have been formed via AOM, fueled by fluids from the underlying mud  
363 diapir.

364 Other carbonate samples from the Al Gacel MV (i.e. D10-R3 and D11-R8) probably have also been formed due  
365 to AOM as they are isotopically depleted as well (δ<sup>13</sup>C values between ca. –25 and –15 ‰, **Fig. 9, Table 3**).  
366 However, no active gas bubbling was observed during sampling, even though both samples still contain open voids  
367 which could form pathways for fluids. Several characteristics of these voids (e.g. dark halos formed by pyrite,  
368 brownish margins due to organic matter enrichments) are very similar to those of methane-derived carbonate  
369 conduits (cf. Reitner et al., 2015). This could imply that the intensity of hydrocarbon-rich seepage and  
370 consequently AOM, may have fluctuated through time. This is in good accordance with the relatively low dominance  
371 of crocetane and PMI in a carbonate sampled from the summit of Al Gacel MV (D11-R8; **Fig. 10**). The moderately  
372 depleted δ<sup>13</sup>C values of crocetane/phytane and PMI in this sample (–57.2 ‰ and –74.3 ‰, respectively; **Table 4**)  
373 could be due to mixing effects and are thus also in agreement with varying intensities of AOM in the environment.  
374 The presence of only few AOM-related DNA sequences (**Fig. 11**) and partly oxidized pyrites in the carbonate  
375 D10-R3 from the base of the Al Gacel MV (**Fig. 8, A–B**) are well in line with this scenario.

376 There is no evidence for eruptive extrusions of muddy materials at the coral ridges. In the Southern Pompeia Coral  
377 Ridge (**Fig. 3**), diapirs appear to rather promote an upward migration of hydrocarbon-rich fluids in a divergent  
378 way throughout a more extensive seabed area. This results in a continuous and diffused seepage, which promotes  
379 the occurrence of AOM and the formation of MDACs at the base of the ridges, related to the sulphate-methane  
380 transition zone (SMTZ) (Boetius et al., 2000; Hinrichs and Boetius, 2002; González et al., 2012a). This is in good  
381 accordance with the detection of methane (80 – 83 nM) at the Northern Pompeia Coral Ridge and the presence of  
382 sulfide-oxidizing bacterial mats and shells of dead chemosynthetic bivalves at the western part of the ridge (**Fig.**  
383 **6, A**). Likewise, the CWC Mounds Field surrounding the Southern Pompeia Coral Ridge (**Fig. 3**) is thoroughly  
384 characterized by micro-seeps, due to ascending fluids from OPs through low-angle faults. This type of focused  
385 seepage may promote formation of MDAC pavements in deeper layers of the sediments (**Fig. 3**), similar to coral

386 ridges along the Pen Duick Escarpment (Wehrmann et al., 2011). The generation of MDAC-hotspots at sites of  
387 such seepage also explain the geometry of the downward tapering cones (Fig. 3).

#### 388 4.2. Ecological meaning of hydrocarbon-rich seepage for CWCs

389 Our data suggests contemporaneous micro-seepage and CWC growth in the Pompeia Province (e.g. Fig. 4, B).  
390 This relationship has also been observed elsewhere, e.g. in the North Sea and off Mid Norway (Hovland, 1990;  
391 Hovland & Thomsen, 1997), and the Angola margin (Le Guilloux et al., 2009). Corals utilize  $\text{HCO}_3^-$  deriving from  
392 both the environment and the internal production of  $\text{CO}_2$  for skeleton biomineralization (Swart, 1983; Zoccola et  
393 al., 2015; Nakamura et al., 2018). Hence, a potential utilization of methane as a carbon source should be reflected  
394 in the  $\delta^{13}\text{C}$  signatures of their skeletons. However, scleractinian fragments recovered from the Al Gacel MV  
395 (embedded in carbonates D10-R3 and D11-R8, from the base and summit of the volcano, respectively) and the  
396 Northern Pompeia Coral Ridge (D03-B1, necrotic part of a living *Madrepora oculata*) displayed barely depleted  
397  $\delta^{13}\text{C}$  values (ca.  $-8$  to  $-1$  ‰; Fig. 9; Table 3), close to the  $\delta^{13}\text{C}$  of marine seawater ( $0 \pm 3$  ‰, e.g. Hoefs, 2015).  
398 These values do not support a significant uptake of methane-derived carbon by the CWCs and thus a direct trophic  
399 dependency as previously proposed (Hovland, 1990). Furthermore, the only DNA in sample D03-B1 that could  
400 be attributed to a potential methanotrophic endosymbiont (ASV\_189; Rodrigues et al., 2013) occurred in minor  
401 amounts and most likely represents contamination from the environment or during sampling. It appears therefore  
402 more likely that the CWCs feed on a mixture of phytoplankton, zooplankton and dissolved organic matter as  
403 previously proposed for ones in other regions (Kiriakoulakis et al., 2005; Duineveld et al., 2007; Becker et al.,  
404 2009; Liebetrau et al., 2010). This is in good accordance with the presence of DNA from various common archaeal  
405 and bacterial taxa (e.g. Acidobacteria, Actinobacteria, Candidatus *Nitrosopumilus*, *Cenarchaeum sp.*) and some  
406 potential members of the corals' holobiont (e.g. Enterobacteria, Verrucomicrobia, *Nitrosococcus sp.*) (Sorokin,  
407 1995; Rådecker et al., 2015; Webster et al., 2016) in sample D03-B1 (Fig. 11). Taken together, there is no evidence  
408 that CWCs in the working area harbor microbial symbionts which potentially could utilize the hydrocarbon-rich  
409 fluids. However, future analyses on living coral-tissue will be important to verify this conclusion.

410 CWC development and hydrocarbon-rich seepage appear to be rather linked *via* the formation of MDAC deposits,  
411 which provide the hard substrata needed for CWC larval settlement (e.g. Díaz-del-Río et al., 2003; Van Rooij et  
412 al., 2011; Magalhães et al., 2012; Le Bris et al., 2016; Rueda et al., 2016). If too severe, however, fluid flow and  
413 associated metabolic processes can result in local conditions that are lethal to CWCs (see 4.3). Moreover, AOM  
414 fueled by fluid flow can also cause an entombment of the CWCs by MDACs (Wienberg et al., 2009; Wienberg &  
415 Titschack, 2015), as observed in D10-R3 and D11-R8 carbonates from the Al Gacel MV (Figs. 7 and 9; Tables 3  
416 and 4). It is therefore not surprising that large CWC systems in the Pompeia Province are always linked to  
417 structures that are affected by rather mild, non-eruptive seepage (i.e. the extinct MV, the coral ridges and the CWC  
418 Mound Fields: Figs. 3 and 6). The observation that these systems are in large parts “coral graveyards” (Fig. 6, B–  
419 D), similar to other areas in the Gulf of Cádiz (see Foubert et al., 2008; Wienberg et al., 2009), may be explained  
420 by a post-glacial decrease in current strength (Foubert et al., 2008). In the light of our findings, however, they  
421 could also have been negatively affected by periods of intensive seepage during higher tectonic activity. Future  
422 studies are important to test this hypothesis in greater detail.

#### 423 4.3. Spatio-temporal co-existence of CWCs and chemosynthetic organisms — the buffer effect

424 As discussed above, MDAC deposits are ecologically beneficial for CWCs, as they serve as optimal substrata even  
 425 when seepage is still present (e. g. Hovland, 1990; Hovland & Thomsen, 1997; Le Guilloux et al., 2009; this study).  
 426 Severe hydrocarbon-rich seepage, however, is ecologically stressful for the corals. Particularly, fluid- and AOM-  
 427 derived hydrogen sulfide is considered problematic because of its role in coral necrosis (Myers & Richardson,  
 428 2009; García et al., 2016) and carbonate dissolution effects (Wehrmann et al., 2011). Corals appear to be  
 429 physiologically tolerant to various of these environmental stressors such as low oxygen concentrations and  
 430 acidification (e. g. Dodds et al., 2007; Form & Riebesell, 2012; McCulloch et al., 2012; Movilla et al., 2014).  
 431 Hydrogen sulfides can furthermore efficiently be buffered through the reaction with Fe-(oxyhydro)-oxides or Fe<sup>2+</sup>  
 432 dissolved in pore waters, ultimately forming pyrite (Wehrmann et al., 2011). It appears that the combination of  
 433 these ecological capabilities plus certain environmental factors allows CWCs to thrive in areas affected by  
 434 hydrocarbon seepage.  
 435 Hydrogen sulfides can efficiently be buffered through the reaction with Fe-(oxyhydro)-oxides or Fe<sup>2+</sup> dissolved in  
 436 pore waters, ultimately forming pyrite (Wehrmann et al., 2011). Fe-(oxyhydro)-oxides nodules have previously  
 437 been observed in the Iberian and Moroccan margins (González et al., 2009; 2012b), but not in the Pompeia  
 438 Province. Instead, sulfide-oxidizing bacteria living in symbiosis with invertebrates (e.g. siboglinid worms:  
 439 Petersen & Dubilier, 2009) (Fig. 5, D) and thriving in mats (Fig. 4, C; Fig. 6, A) were particularly prominent along  
 440 this region. These microbes withdraw reduced sulfur species through their metabolic activity, thus forming a  
 441 biological buffer. Likewise, microbially mediated AOM substantially increases carbonate alkalinity at active sites,  
 442 thereby providing a buffer against acidification on a local scale (e.g., in the active pockmark from the Al Gacel  
 443 MV where seawater pH was 7.85, see section 3.2). These microbes may form a biological buffer by withdrawing  
 444 reduced sulfur species through their metabolic activity. Likewise, the consumption of methane and sulfate by  
 445 AOM microorganisms at active sites also contribute to CWCs colonization of the carbonates by reducing  
 446 environmental acidification (seawater pH was 7.85 in the active pockmark from the Al Gacel MV; see section  
 447 3.2).  
 448 We propose that this-such biological buffers provides a further ecological linkage between hydrocarbon-rich  
 449 seepage and cold-water corals along the Pompeia Province ("buffer effect model": Fig. 12). This model explains  
 450 the observed co-existence of non-chemosynthetic corals (e.g. on top of D10 R7 carbonate: Fig. 5) with AOM-  
 451 microorganisms and chemosynthetic sulfide oxidizing organisms at pockmark sites at the Al Gacel MV (Fig. 12,  
 452 A). At the same time, it is in line with associations of sulfide oxidizing bacterial mats, scleractinian corals, and  
 453 other non-chemosynthetic octocorals at diapiric ridges and coral mounds in the Northern Pompeia Coral Ridge  
 454 (Fig. 12, B, C). The impact and exact capacity of this biological buffer, however, remains elusive and must be  
 455 evaluated in future studies.

## 456 5. Conclusions

457 Cold-water coral occurrences in the Pompeia Province (Gulf of Cádiz) are typically linked to hydrocarbon-seep  
 458 structures like mud volcanoes and diapirs. The irregular topography of these structures affects bottom water-  
 459 currents which supply nutrients to the corals. A further ecological benefit is the seepage-fueled formation of  
 460 authigenic carbonates, which provide ideal substrates for coral larvae settlement. Cold-water corals therefore take  
 461 indirectly advantages of seepage-related conditions, instead of feeding from the seeped fluids, such as sulfide and  
 462 methane. However, increased fluid seepage appears to be ecologically disadvantageous as evidenced by corals

Con formato: Fuente: (Predeterminada) Times New Roman, Sin Resaltar

Con formato: Sin Resaltar

Con formato: Fuente: (Predeterminada) Times New Roman, Sin Resaltar

Con formato: Sin Resaltar

Con formato: Fuente: (Predeterminada) Times New Roman, Sin Resaltar

Con formato: Sin Resaltar

Con formato: Fuente: (Predeterminada) Times New Roman

Con formato: Fuente: (Predeterminada) Times New Roman, Sin Resaltar

Con formato: Fuente: (Predeterminada) Times New Roman

Con formato: Fuente: (Predeterminada) Times New Roman

Con formato: Sin Resaltar

Con formato: Fuente: (Predeterminada) Times New Roman

Con formato: Fuente: 10 pts

463 embedded in some of the carbonates. Consequently, cold-water coral growth in these habitats depends directly on  
464 seepage intensity and how these fluids are drained onto the seafloor (i.e. eruptive, focused, diffused or dripping-  
465 like). Cold-water coral growth appears to be furthermore supported by the microbial-mediated removal of seepage-  
466 related toxic substances (e. g., reduced sulfur species through sulfide-oxidizing bacteria) and shaping of  
467 environmental conditions (e. g., pH-buffering through AOM). This biological buffer is possibly crucial to keep  
468 conditions favorable for the growth of cold-water corals in the studied area, particularly in times of increased fluid  
469 seepage.

#### 470 **Author contribution**

471 Blanca Rincón-Tomás, Dominik Schneider and Michael Hoppert carried out the microbial analysis. Jan-Peter  
472 Duda carried out the biomarker analysis. Luis Somoza and Teresa Medialdea processed seismic and bathymetric  
473 data. Pedro Madureira processed ROV data. Javier González and Joachim Reitner carried out the petrographic  
474 analysis. Esther Santofimia and Enrique López-Pamo carried out the pore-water and seawater analysis. Joachim  
475 Reitner carried out the stable isotopic analysis. Blanca Rincón-Tomás prepared the manuscript with  
476 contributions from all co-authors.

#### 477 **Competing interests**

478 The authors declare that they have no conflict of interest.

#### 479 **Acknowledgments**

480 The authors thank the captain and the crew on board the R/V Sarmiento de Gamboa, as well as the UTM (Unidad  
481 de Tecnología Marina), that have been essential for the success of this paper. Data obtained on board is collected  
482 in the SUBVENT-2 cruise, which can be found in the IGME archive. This work was supported by the Spanish  
483 project SUBVENT (CGL2012-39524-C02) and the project EXPLOSEA (CTM2016-75947) funded by the Spanish  
484 Ministry of Science, Innovation and Universities.

#### 485 **References**

- 486 Ahmed, M. and George, S.C.: Changes in the molecular composition of crude oils during their preparation for GC  
487 and GC-MS analyses, *Org. Geochem.*, 35, 137–155, doi:10.1016/j.orggeochem.2003.10.002, 2004.
- 488 Becker, E. L., Cordes, E. E., Macko, S. A., and Fisher, C. R.: Importance of seep primary production to *Lophelia*  
489 *pertusa* and associated fauna in the Gulf of Mexico, *Deep-sea Res Pt I*, 56(5), 786–800,  
490 doi:10.1016/j.dsr.2008.12.006, 2009.
- 491 Birgel, D., Thiel, V., Hinrichs, K. U., Elvert, M., Campbell, K. A., Reitner, J., Farmer, J. D., and Peckmann, J.:  
492 Lipid biomarker patterns of methane-seep microbialites from the Mesozoic convergent margin of  
493 California, *Org. Geochem.*, 37(10), 1289–1302, doi:10.1016/j.orggeochem.2006.02.004, 2006.
- 494 Boetius, A., Ravensschlag, K., Schubert, C. J., Rickert, D., Widdel, F., Gieseke, A., Amann, R., Jørgensen, B. B.,  
495 Witte, U., and Pfannkuche, O.: A marine microbial consortium apparently mediating anaerobic oxidation  
496 of methane, *Nature*, 407 (6804), 623–626, doi:10.1038/35036572, 2000.

497 Callahan, B., MacMurdie, P. J., and Holmes, S. O.: Exact sequence variants should replace optional taxonomic  
498 units in marker-gene data analysis, *ISME J.*, 11, 2639–2643, doi:10.1038/ismej.2017.119, 2017.

499 Caporaso, J.G., Kuczynski, J., Stombaugh, J., Bittinger, K., Bushman, F.D., Costello, E.K., Fierer, N., González-  
500 Peña, A., Goodrich, J. K., Gordon, J. I., Huttley, G. A., Knights, D., Koenig, J. E., Lozupone, C. A.,  
501 McDonald, D., Muegge, B. D., Pirrung, M., Reeder, J., Sevinsky, J. R., Turnbaugh, P. J., Walters, W. A.,  
502 Widmann, J., Yatsunenko, T., Zaneveld, J., and Knight, R.: QIIME allows analysis of high-throughput  
503 community sequencing data, *Nat. Methods*, 7, 335–336, doi:10.1038/nmeth.f.303, 2010.

504 Cordes, E., Arnaud-Haond, S., Bergstad, O., da Costa Falcão, A. P., Freiwald, A., Roberts, J. M., and Bernal, P.:  
505 Cold water corals, in: *The First Global Integrated Marine Assessment, World Ocean Assessment I*, United  
506 Nations, Cambridge University Press, Cambridge, United Kingdom, 2016.

507 Díaz-del-Río, V., Somoza, L., Martínez-Frías, J., Mata, M. P., Delgado, A., Hernandez-Molina, F. J., ..., Vázquez,  
508 J. T.: Vast fields of hydrocarbon-derived carbonate chimneys related to the accretionary  
509 wedge/olistostrome of the Gulf of Cádiz, *Mar. Geol.*, 195, 177–200, doi:10.1016/S0025-3227(02)00687-  
510 4, 2003.

511 Dodds, L. A., Roberts, J. M., Taylor, A. C., and Marubini, F.: Metabolic tolerance of the cold-water coral *Lophelia*  
512 *pertusa* (Scleractinia) to temperature and dissolved oxygen change. *J. Exp. Mar. Biol. Ecol.*, 349(2), 205–  
513 214, doi:10.1016/j.jembe.2007.05.013, 2007.

514 Dorschel, B., Hebbeln, D., Foubert, A., White, M., and Wheeler, A. J.: Hydrodynamics and cold-water coral facies  
515 distribution related to recent sedimentary processes at Galway Mound west of Ireland, *Mar. Geol.*, 244,  
516 184–195, doi:10.1016/j.margeo.2007.06.010, 2007.

517 Duineveld, G. C., Lavaleye, M. S., Bergman, M. J., De Stigter, H., and Mienis, F.: Trophic structure of a cold-  
518 water coral mound community (Rockall Bank, NE Atlantic) in relation to the near-bottom particle supply  
519 and current regime, *B. Mar. Sci.*, 81 (3), 449–467, 2007.

520 Dullo, W. C., Flögel, S., and Rüggerberg, A.: Cold-water coral growth in relation to the hydrography of the Celtic  
521 and Nordic European continental margin, *Mar. Ecol. Prog. Ser.*, 371, 165–176, doi:10.3354/meps07623,  
522 2008.

523 Dunham, R. J., 1962, Classification of carbonate rocks according to their depositional texture, in: *Classification*  
524 *of Carbonate Rocks*, Ham, W. E. (Eds.), American Association of Petroleum Geologists Memoir 1, Tulsa,  
525 OK, 108–121, 1962.

526 Edgar, R. C.: USEARCH. <http://www.drive5.com/usearch>. 2010.

527 Egelkamp, R., Schneider, D., Hertel, R., and Daniel, R.: Nitrile-Degrading Bacteria Isolated from Compost, *Front.*  
528 *Environ. Sci.*, 5, doi: 10.3389/fenvs.2017.00056, 2017.

529 Embry III, A. F., and Klován, J. E.: A late Devonian reef tract on northeastern Banks Island, NWT, B. *Can. Petrol.*  
530 *Geol.*, 19(4), 730–781, 1971.

531 Form, A. U., and Riebesehl, U.: Acclimation to ocean acidification during long-term CO2 exposure in the cold-  
532 water coral *Lophelia pertusa*. *Glob. Change Biol.*, 18(3), 843–853, doi: 10.1111/j.1365-  
533 2486.2011.02583.x, 2012.

534 Foubert, A., Depreiter, D., Beck, T., Maignien, L., Pannemans, B., Frank, N., Blamart, D., and Henriët, J.:  
535 Carbonate mounds in a mud volcano province off north-west Morocco: key to processes and controls,  
536 *Mar. Geol.*, 248, 74–96, doi: 10.1016/j.margeo.2007.10.012, 2008.

Con formato: Fuente: Cursiva

Con formato: Inglés (Estados Unidos)

Con formato: Fuente: Cursiva, Inglés (Estados Unidos)

Con formato: Inglés (Estados Unidos)

Con formato: Alemán (Alemania)

Con formato: Fuente: 10 pto

537 Garcia, G. D., Santos, E. D. O., Sousa, G. V., Zingali, R. B., Thompson, C. C., and Thompson, F. L.:  
538 Metaproteomics reveals metabolic transitions between healthy and diseased stony coral *Mussismilia*  
539 *braziliensis*, *Mol. Ecol.*, 25(18), 4632–4644, doi:10.1111/mec.13775, 2016.

540 Goedert, J. L., and Peckmann, J.: Corals from deep-water methane-seep deposits in Paleogene strata of Western  
541 Oregon and Washington, U.S.A., in: *Cold-water corals and Ecosystems*, Freiwald, A., and Roberts, J. M.  
542 (eds.), Springer-Verlag, Berlin Heidelberg, 27–40, 2005.

543 Gomes-Sumida, P.Y., Yoshinaga, M.Y., Saint-Pastous Madureira, L.A., and Hovland, M.: Seabed pockmarks  
544 associated with deep water corals off SE Brazilian continental slope, Santos Basin, *Mar. Geol.*, 207, 159–  
545 167, doi:10.1016/j.margeo.2004.03.006, 2004.

546 González, F. J., Somoza, L., Lunar, R., Martínez-Frías, J., Martín Rubí, J. A., Torres, T., Ortiz, J. E., Díaz-del-  
547 Río, V., Pinheiro, L. M., and Magalhães, V. H.: Hydrocarbon-derived ferromanganese nodules in  
548 carbonate mud mounds from the Gulf of Cádiz: mud-breccia sediments and clasts as nucleation sites,  
549 *Mar. Geol.*, 261, 64–81, doi:10.1016/j.margeo.2008.11.005, 2009.

550 González, F. J., Somoza, L., León, R., Medialdea, T., de Torres, T., Ortiz, J. E., Martínez-Frías, J., and Merinero,  
551 R.: Ferromanganese nodules and micro-hardgrounds associated with the Cádiz Contourite Channel (NE  
552 Atlantic): Palaeoenvironmental records of fluid venting and bottom currents, *Chem. Geol.*, 310–311, 56–  
553 78, doi: 10.1016/j.chemgeo.2012.03.030, 2012a.

554 González, F. J., Somoza, L., Medialdea, T., León, R., Torres, T., Ortiz, J. E., and Martín-Rubí, J. A.: Discovery of  
555 ferromanganese hydrocarbon-related nodules associated with the Meknes mud volcano (Western  
556 Moroccan margin). European Geoscience Union 2012 (EGU2012). Viena (Austria). *Geophys. Res. Abs.*  
557 vol. 14, EGU2012-12306, 2012b.

558 Hebbeln, D., Van Rooij, D., and Wienberg, C.: Good neighbours shaped by vigorous currents: cold-water coral  
559 mounds and contourites in the North Atlantic, *Mar. Geol.*, 378, 171–185,  
560 doi:10.1016/j.margeo.2016.01.014, 2016.

561 Hensen, C., Nuzzo, M., Hornibrook, E., Pinheiro, L.M., Bock, B., Magalhães, V.H., and Brückmann, W.: Sources  
562 of mud volcano fluids in the Gulf of Cádiz — indications for hydrothermal imprint, *Geochim.*  
563 *Cosmochim. Ac.*, 71 (5), 1232–1248, doi:10.1016/j.gca.2006.11.022, 2007.

564 Hinrichs, K. -U., and Boetius, A.: The anaerobic oxidation of methane: new insights in microbial ecology and  
565 biogeochemistry, in: *Ocean Margin Systems*, Wefer, G., Billett, D., Hebbeln, D., Jørgensen, B.B.,  
566 Schlueter, M., Van Weering, T. (Eds.), Springer-Verlag, Berlin, 457–477, 2002.

567 Hinrichs, K. -U., Hayes, J. M., Sylva, S. P., Brewer, P. G., and De Long, E. F.: Methane-consuming archaeobacteria  
568 in marine sediments, *Nature*, 398, 802–805, doi:10.1038/19751, 1999.

569 Hoefs, J.: *Stable Isotope Geochemistry*, Springer, Berlin, 2015.

570 Hovland, M.: Do carbonate reefs form due to fluid seepage?, *Terra Nova*, 2, 8–18, doi:10.1111/j.1365-  
571 3121.1990.tb00031.x, 1990.

572 Hovland, M., Jensen, S., and Indreien, T.: Unit pockmarks associated with *Lophelia* coral reefs off mid-Norway:  
573 more evidence of control by ‘fertilizing’ bottom currents, *Geo-Mar. Lett.*, 32 (5–6), 545–554,  
574 doi:10.1007/s00367-012-0284-0, 2012.

575 Hovland, M., Mortensen, P. B., Brattegard, T., Strass, P., and Rokoengen, K.: Ahermatypic coral banks off mid-  
576 Norway: evidence for a link with seepage of light hydrocarbons, *Palaios*, 13, 189–200, doi:10.1043/0883-  
577 1351(1998)013<0189:ACBOME>2.0.CO;2, 1998.

- 578 Hovland, M., and Thomsen, E.: Cold-water corals — are they hydrocarbon seep related?, *Mar. Geol.*, 137, 159–  
579 164, doi:10.1016/S0025-3227(96)00086-2, 1997.
- 580 Huvenne, V. A., Masson, D. G., and Wheeler, A. J.: Sediment dynamics of a sandy contourite: the sedimentary  
581 context of the Darwin cold-water coral mounds, Northern Rockall Trough, *Int. J. Earth Sci.*, 98 (4), 865–  
582 884, doi: 10.1007/s00531-008-0312-5, 2009.
- 583 Ivanov, M. K., Akhmetzhanov, A. M., and Akhmanov, G. G.: Multidisciplinary study of geological processes on  
584 the North East Atlantic and Western Mediterranean Margins, in: *Loc. Tech. S.*, 56, UNESCO, 2000.
- 585 Kiriakoulakis, K., Fisher, E., Wolff, G. A., Freiwald, A., Grehan, A., and Roberts, J. M.: Lipids and nitrogen  
586 isotopes of two deep-water corals from the North-East Atlantic: initial results and implications for their  
587 nutrition, in: *Cold-Water Corals and Ecosystems*, Freiwald, A., Roberts, J. M. (Eds.), Erlangen Earth  
588 Conf., Springer, Germany, 715–729, 2005.
- 589 Le Bris, N., Arnaud-Haond, S., Beaulieu, S., Cordes, E. E., Hilario, A., Rogers, A., van de Gaeve, S., and  
590 Watanabe, H.: Hydrothermal Vents and Cold Seeps, in: *The First Global Integrated Marine Assessment*,  
591 United Nations, Cambridge University Press, Cambridge, United Kingdom, 2016.
- 592 Le Guilloux, E., Olu, K., Bourillet, J. F., Savoye, B., Iglésias, S. P., and Sibuet, M.: First observations of deep-sea  
593 coral reefs along the Angola margin, *Deep-sea Res. Pt. II*, 56, 2394–2403,  
594 doi:10.1016/j.dsr2.2009.04.014, 2009.
- 595 Liebetrau, V., Eisenhauer, A., and Linke, P.: Cold seep carbonates and associated cold-water corals at the  
596 Hikurangi Margin, New Zealand: new insights into fluid pathways, growth structures and geochronology,  
597 *Mar. Geol.*, 272, 307–318, doi:10.1016/j.margeo.2010.01.003, 2010.
- 598 León, R., Somoza, L., Medialdea, T., Vázquez, J. T., González, F. J., López-González, N., Casas, D., del Pilar  
599 Mata, M., del Fernández-Puga, C., Giménez-Moreno, C. J., and Díaz-del-Río, V.: New discoveries of  
600 mud volcanoes on the Moroccan Atlantic continental margin (Gulf of Cádiz): morpho-structural  
601 characterization, *Geo-Mar. Lett.*, 32, 473–488, doi:10.1007/s00367-012-0275-1, 2012.
- 602 Magalhães, V. H., Pinheiro, L. M., Ivanov, M. K., Kozlova, E., Blinova, V., Kolganova, J., Vasconcelos, C.,  
603 McKenzie, J. A., Bernasconi, S. M., Kopf, A., Díaz-del-Río, V., González, F. J., and Somoza, L.:  
604 Formation processes of methane-derived authigenic carbonates from the Gulf of Cádiz, *Sediment. Geol.*,  
605 243–244, 155–168, doi:10.1016/j.sedgeo.2011.10.013, 2012.
- 606 Margreth, S., Gennari, G., Rüggeberg, A., Comas, M. C., Pinheiro, L. M., and Spezzferri, S.: Growth and demise  
607 of cold-water coral ecosystems on mud volcanoes in the West Alboran Sea: The messages from planktonic  
608 and benthic foraminifera, *Mar. Geol.*, 282, 26–39, doi:10.1016/j.margeo.2011.02.006, 2011.
- 609 Martin, M.: Cutadapt removes Adapter Sequences from High-Throughput Sequencing Reads, *EMBnet.journal*, 10–  
610 12, doi: 10.14806/ej.17.1.200, 2011.
- 611 [McCulloch, M., Falter, J., Trotter, J., and Montagna, P.: Coral resilience to ocean acidification and global warming](#)  
612 [through pH up-regulation. \*Nat. Clim. Change\*, 2\(8\), 623–627, doi: 10.1038/nclimate1473, 2012.](#)
- 613 Medialdea, T., Somoza, L., Pinheiro, L. M., Fernández-Puga, M. C., Vázquez, J. T., León, R., Ivanov, M. K.,  
614 Magalhães, V., Díaz-del-Río, V., and Vegas, R.: Tectonics and mud volcano development in the Gulf of  
615 Cádiz, *Mar. Geol.*, 261, 48–63, doi:10.1016/j.margeo.2008.10.007, 2009.
- 616 Mortensen, P. B., Hovland, M. T., Fossa, J. H., and Furevik, D. M.: Distribution, abundance and size of *Lophelia*  
617 *pertusa* coral reefs in mid Norway in relation to seabed characteristics, *J. Mar. Biol. Assoc. UK*, 81, 581–  
618 597, doi:10.1017/S002531540100426X, 2001.

Con formato: Inglés (Estados Unidos)

Con formato: Inglés (Estados Unidos)

Con formato: Inglés (Estados Unidos)

Con formato: Fuente: 10 pto

619 Movilla, J., Gori, A., Calvo, E., Orejas, C., López-Sanz, À., Domínguez-Carrió, C., Grinyó, J., and Pelejero, C.:  
620 Resistance of two Mediterranean cold-water coral species to low-pH conditions, *Water*, 6(1), 59–67, 2014.  
621 Myers, J.L., and Richardson, L.L.: Adaptation of cyanobacteria to the sulfide-rich microenvironment of black band  
622 disease of coral, *FEMS Microbiol. Ecol.*, 67, 242–251, doi:10.1111/j.1574-6941.2008.00619.x, 2009.  
623 Nakamura, T., Nadaoka, K., Watanabe, A., Yamamoto, T., Miyajima, T., and Blanco, A. C.: Reef-scale modeling  
624 of coral calcification responses to ocean acidification and sea-level rise, *Coral Reefs*, 37, 2018.  
625 Peckmann, J., Reimer, A., Luth, U., Luth, C., Hansen, B.T., Heinicke, C., Hoefs, J., and Reitner, J.: Methane-  
626 derived carbonates and authigenic pyrite from the northwestern Black Sea, *Mar. Geol.*, 177, 129–150,  
627 doi:10.1016/S0025-3227(01)00128-1, 2001.  
628 Peckmann, J., and Thiel, V.: Carbon cycling at ancient methane-seeps, *Chem. Geol.*, 205 (3), 443–467,  
629 doi:10.1016/j.chemgeo.2003.12.025, 2004.  
630 Petersen, J. M., and Dubilier, N.: Methanotrophic symbioses in marine invertebrates, *Env. Microbiol. Rep.*, 1(5),  
631 319–335, doi:10.1111/j.1758-2229.2009.00081.x, 2009.  
632 Pinheiro, L. M., Ivanov, M. K., Sautkin, A., Akhmanov, G., Magalhães, V. H., Volkonskaya, A., Monteiro, J. H.,  
633 Somoza, L., Gardner, J., Hamouni, N., and Cunha, M. R.: Mud volcanism in the Gulf of Cádiz: results  
634 from the TTR-10 cruise, *Mar. Geol.*, 195, 131–151, doi:10.1016/S0025-3227(02)00685-0, 2003.  
635 Rådecker, N., Pogoreutz, C., Voolstra, C. R., Wiedenmann, J., and Wild, C.: Nitrogen cycling in corals: The key  
636 to understanding holobiont functioning?, *Trends Microbiol.*, 23 (8), 490–497,  
637 doi:10.1016/j.tim.2015.03.008, 2015.  
638 Reitner, J., Gauret, P., Marin, F., and Neuweiler, F.: Automicrites in a modern marine microbialite. Formation  
639 model via organic matrices (Lizard Island, Great Barrier Reef, Australia), *Bull.-Inst. Oceanogr. Monaco*,  
640 14, 237–263, 1995.  
641 Reitner, J., Blumenberg, M., Walliser, E. -O., Schäfer, N., and Duda, J. -P.: Methane-derived carbonate conduits  
642 from the late Aptian of Salinac (Marne Bleues, Vocontian Basin, France): Petrology and biosignatures,  
643 *Mar. Petrol. Geol.*, 66 (3), 641–652, doi:10.1016/j.marpetgeo.2015.05.029, 2015.  
644 Reitner, J., Peckmann, J., Blumenberg, M., Michaelis, W., Reimer, A., and Thiel, V.: Concretionary methane-seep  
645 carbonates and associated microbial communities in Black Sea sediments, *Palaeogeogr., Palaeoclimatol.,*  
646 *Palaeocl.*, 227, 18–30, doi:10.1016/j.palaeo.2005.04.033, 2005.  
647 Roberts, J. M., Long, D., Wilson, J. B., Mortensen, P. B., and Gage, J. D.: The cold-water coral *Lophelia pertusa*  
648 (Scleractinia) and enigmatic seabed mounds along the north-east Atlantic margin: are they related?, *Mar.*  
649 *Pollut. Bull.*, 46, 7–20, doi:10.1016/S0025-326X(02)00259-X, 2003.  
650 Roberts, J. M., Wheeler, A. J., and Freiwald, A.: Reefs of the deep: the biology and geology of cold-water coral  
651 ecosystems, *Science*, 312 (5773), 543–547, doi:10.1126/science.1119861, 2006.  
652 Roberts, J. M., Wheeler, A., Freiwald, A., and Cairns, S. (Eds.): *Cold-water corals: the biology and geology of*  
653 *deep-sea coral habitats*, Cambridge University Press, Cambridge, United Kingdom, 2009.  
654 Rodrigues, C. F., Cunha, M. R., Génio, L., and Duperron, S.: A complex picture of associations between two host  
655 mussels and symbiotic bacteria in the Northeast Atlantic, *Naturwissenschaften*, 100, 21–31,  
656 doi:10.1007/s00114-012-0985-2, 2013.  
657 Rogers, A. D.: The Biology of *Lophelia pertusa* (Linnaeus 1758) and other Deep-Water Reef-Forming Corals and  
658 Impacts from Human Activities, *Int. Rev. Hydrobiol.*, 84 (4), 315–406, doi:10.1002/iroh.199900032,  
659 1999.

Con formato: Inglés (Estados Unidos)

Con formato: Inglés (Estados Unidos)

Con formato: Fuente: 10 pto

660 Rueda, J. L., González-García, E., Krutzky, C., López-Rodríguez, J., Bruque, G., López-González, N., Palomino,  
661 D., Sánchez, R. F., Vázquez, J. T., Fernández-Salas, L. M., and Díaz-del-Río, V.: From chemosynthetic-  
662 based communities to cold-water corals: Vulnerable deep-sea habitats of the Gulf of Cádiz, *Mar.*  
663 *Biodiver.*, 46, 473–482, doi:10.1007/s12526-015-0366-0, 2016.

664 Sánchez-Guillamón, O., García, M. C., Moya-Ruiz, F., Vázquez, J. T., Palomino, D., Fernández-Puga, M. C., and  
665 Sierra, A.: A preliminary characterization of greenhouse gas (CH<sub>4</sub> and CO<sub>2</sub>) emissions from Gulf of Cádiz  
666 mud volcanoes, VIII Symposium MIA15, 2015.

667 Somoza, L., Ercilla, G., Urgorri, V., León, R., Medialdea, T., Paredes, M., González, F. J., and Nombela, M. A.:  
668 Detection and mapping of cold-water coral mounds and living *Lophelia* reefs in the Galicia Bank, Atlantic  
669 NW Iberia margin, *Mar. Geol.*, 349, 73–90, doi:10.1016/j.margeo.2013.12.017, 2014.

670 Somoza, L., León, R., Ivanov, M. Fernández-Puga, M. C., Gardner, J. M., Hernández-Molina, F. J., Pinheiro, L.  
671 M., Rodero, J., Lobato, A., Maestro, A., Vázquez, J. T., Medialdea, T., and Fernández-Salas, L. M.:  
672 Seabed morphology and hydrocarbon seepage in the Gulf of Cádiz mud volcano area: Acoustic imagery,  
673 multibeam and ultra-high resolution seismic data, *Mar. Geol.*, 195, 153–176, doi:10.1016/S0025-  
674 3227(02)00686-2, 2003.

675 Sorokin, Y. I.: Coral reef ecology, Springer, Germany, 1995.

676 Suess, E. and Whiticar, M. J.: Methane-derived CO<sub>2</sub> in pore fluids expelled from the Oregon subduction zone,  
677 *Palaeogeogr., Palaeoclimatol., Palaeocl.*, 71, 119–136, doi:10.1016/0031-0182(89)90033-3, 1989.

678 Swart, P. K.: Carbon and Oxygen Isotope Fractionation in Scleractinian Corals: a Review, *Earth-Sci. Rev.*, 19,  
679 51–80, 1983.

680 Thiel, V., Peckmann, J., Seifert, R., Wehrung, P., Reitner, J., and Michaelis, W.: Highly isotopically depleted  
681 isoprenoids: molecular markers for ancient methane venting, *Geochim. Cosmochim. Ac.*, 63, 3959–3966,  
682 doi:10.1016/S0016-7037(99)00177-5, 1999.

683 Thiel, V., Peckmann, J., Richnow, H.-H., Luth, U., Reitner, J., and Michaelis, W.: Molecular signals for anaerobic  
684 methane oxidation in Black Sea seep carbonates and a microbial mat, *Mar. Chem.* 73, 97–112,  
685 doi:10.1016/S0304-4203(00)00099-2, 2001.

686 Thiem, Ø., Ravagnan, E., Fosså, J. H., and Berntsen, J.: Food supply mechanisms for cold- water corals along a  
687 continental shelf edge, *J. Marine Syst.*, 26, 1481–1495, doi:10.1016/j.jmarsys.2005.12.004, 2006.

688 Vadorpe, T., Martins, I., Vitorino, J., Hebbeln, D., García-García, M., and Van Rooij, D.: Bottom currents and  
689 their influence on the sedimentation pattern in the El Arraiche mud volcano province, southern Gulf of  
690 Cádiz, *Mar. Geol.*, 378, 114–126, doi:10.1016/j.margeo.2015.11.012, 2016.

691 Vadorpe, T., Wienberg, C., Hebbeln, D., Van den Berghe, M., Gaide, S., Wintersteller, P., and Van Rooij, D.:  
692 Multiple generations of buried cold-water coral mounds since the Early-Middle Pleistocene Transition in  
693 the Atlantic Moroccan Coral Province, southern Gulf of Cádiz, *Palaeogeogr., Palaeoclimatol., Palaeocl.*,  
694 485, 293–304, doi:10.1016/j.palaeo.2017.06.021, 2017.

695 Van Rensbergen, P., Depreiter, D., Pannemans, B., Moerkerke, G., Van Rooij, D., Marsset, B., Akhmanov, G.,  
696 Blinova, V., Ivanov, M., Rachidi, M., Magalhães, V., Pinheiro, L., Cunha, M., and Henriot, J.P.: The  
697 Arraiche mud volcano field at the Moroccan Atlantic slope, Gulf of Cádiz, *Mar. Geol.*, 219, 1–17,  
698 doi:10.1016/j.margeo.2005.04.007, 2005.

699 Van Rooij, D., Blamart, D., De Mol, L., Mienis, F., Pirlet, H., Whermann, L. M., ..., Henriët, J. -P.: Cold-water  
700 coral mounds on the Pen Duick Escarpment, Gulf of Cádiz: The MiCROSYSTEMS project approach,  
701 *Mar. Geol.*, 282, 102–117, doi:10.1016/j.margeo.2010.08.012, 2011.

702 Watling, L., France, S. C., Pante, E., and Simpson, A.: Biology of Deep-Water Octocorals, in: *Advances in Marine*  
703 *Biology Volume 60*, Lesser, M. (Eds.), Academic Press, London, United Kingdom, 41–122, 2011.

704 Webster, N. S., Negri, A. P., Botté, E. S., Laffy, P. W., Flores, F., Noonan, S., Schmidt, C., and Uthicke, S.: Host-  
705 associated coral reef microbes respond to the cumulative pressures of ocean warming and ocean  
706 acidification *Sci. Rep.-UK*, 6, doi:10.1038/srep19324, 2016.

707 Wheeler, A. J., Beyer, A., Freiwald, A., de Haas, H., Huvenne, V. A., Kozachenko, M., Olu-Le Roy, K.,  
708 and Opderbecke, J.: Morphology and environment of cold-water coral carbonate mounds on the NW  
709 European margin, *Int. J. Earth Sci.*, 96, 37–56, doi:10.1007/s00531-006-0130-6, 2007.

710 Wehrmann, L. M. Templer, S. P., Brunner, B., Bernasconi, S. M., Maignien, L., and Ferdelman, T. G.: The imprint  
711 of methane seepage on the geochemical record an early diagenetic processes in cold-water coral mounds  
712 on Pen Duick Escarpment, Gulf of Cádiz, *Mar. Geol.*, 118–137, doi:10.1016/j.margeo.2010.08.005, 2011.

713 Wienberg, C., Hebbeln, D., Fink, H. G., Mienis, F., Dorschel, B., Vertino, A., López-Correa, M., and Freiwald,  
714 A.: Scleractinian cold-water corals in the Gulf of Cádiz—first clues about their spatial and temporal  
715 distribution, *Deep-sea Res. Pt. I*, 56 (10), 1873–1893, doi:10.1016/j.dsr.2009.05.016, 2009.

716 Wienberg, C., and Titschack, J.: Framework-forming scleractinian cold-water corals through space and time: a  
717 late Quaternary North Atlantic perspective, in: *Marine Animal Forests: The Ecology of Benthic*  
718 *Biodiversity Hotspots*, Rossi, S., Bramanti, L., Gori, A., and Orejas, C. (Eds.), Springer, Cham,  
719 Switzerland, 1–34, 2015.

720 Yilmaz, P., Parfrey, L.W., Yarza, P., Gerken, J., Pruese, E., Quast, C., Schweer, T., Peplies, J., Ludwig, W., and  
721 Glöckner, F. O.: The SILVA and ‘All-species Living Tree Project (LTP)’ taxonomic frameworks, *Nucleic*  
722 *Acids Res.*, 42, D643–D648, doi:10.1093/nar/gkt1209, 2014.

723 Zhang, J., Kobert, K., Flouri, T., and Stamatakis, A.: PEAR: a fast and accurate Illumina Paired-End reAd  
724 merger, *Bioinformatics*, 30 (5), 614–620, doi:10.1093/bioinformatics/btt593, 2014.

725 Zoccola, D., Ganot, P., Bertucci, A., Caminit-Segonds, N., Techer, N., Voolstra, C. R., Aranda, M., Tambutté, E.,  
726 Allemand, D., Casey, J. R., and Tambutté, S.: Bicarbonate transporters in corals point towards a key step  
727 in the evolution of cnidarian calcification, *Sci. rep.-UK*, 5, 2015.

728  
729  
730  
731  
732  
733  
734  
735  
736  
|

737  
738  
739  
740  
741  
742  
743  
744  
745  
746  
747  
748  
749  
750

**Table 1.** General description and characterization of recovered samples for this study in the Al Gacel MV and Northern Pompeia ~~Province~~Coral Ridge. Please note that samples D10-R3 and D11-R8 were carbonates with embedded corals (see Fig. 7 for more details).

Con formato: Fuente: Negrita

	Site description	Coordinates	Depth (m)	Type	Sample
Al Gacel MV	Base of volcano characterized by non-chemosynthetic fauna	35° 26.51' N -6° 58.22' W	850 – 890	Carbonate	D10-R3
	Active pockmark	35° 26.47' N -6° 58.27' W	790	Carbonate	D10-R7
				Water	D10-N4
					D10-C5
	Summit with metric carbonate blocks	35° 26.48' N -6° 58.35' W	763	Carbonate	D11-R8
				Water	D11-N9
	35° 26.48' N -6° 58.37' W	760			D11-C10
Northern Pompeia Coral Ridge	Sulfide-oxidizing bacterial mats and shells of chemosynthetic bivalves	35° 26.77' N -6° 59.94' W	829	Necrotic fragment of a living <i>Madrepora oculata</i> coral	D03-B1

751  
752

**Table 2.** In-situ water variables measured during sampling with ROV sensors.

	D10-R3	D10-R7	D11-R8	D03-B1

20 Con formato: Fuente: 10 pto

Temperature (°C)	10.07	10.5	10.02	10.04 – 10.05
Conductivity (mS/cm)	39.13 – 39.62	39.05 – 39.43	-	-
Salinity (ppt)	-	-	35.56 – 35.86	35.67 – 35.91
Saturation of dissolved oxygen (%)	53.64 – 54.69	54.02 – 54.35	51.95 – 53.92	52.46 – 56.22
Dissolved oxygen (mg/l)	4.81 – 4.90	4.85 – 4.88	4.66 – 4.84	4.71 – 5.09
Density (kg/m <sup>3</sup> )	31.03 – 31.42	30.94 – 31.24	30.92 – 31.08	31.26 – 31.41

753  
754 **Table 3.** On site measurements of soluble Fe<sup>2+</sup> and S<sup>2+</sup> values from seawater and pore-water. Please note that  
755 samples D10-C5, D10-C8 and D10-N4 were taken from the same site as the authigenic carbonate D10-R7 (see  
756 **Fig. 2**). d.l. = detection limit.

Sample	Type	Fe <sup>2+</sup> (μM)	S <sup>2+</sup> (μM)	pH	ORP (mV)
D10-C5 (0 – 6 cm)	Pore-water	0.94	< d.l.	-	-
D10-C5 (6 – 16 cm)		1.27	< d.l.	-	-
D10-C8 (0 – 6 cm)		2.70	< d.l.	-	-
D10-C8 (6 – 16 cm)		1.74	0.23	-	-
D10-N4	Sea-water	0.57	< d.l.	7.88	136
D11-C10 (0 – 5 cm)	Pore-water	2.39	< d.l.	-	-
D11-C10 (5 – 15 cm)		5.32	0.47	-	-
D11-N9	Seawater	0.31	< d.l.	7.85	257

Tabla con formato

757  
758  
759  
760  
761  
762  
763  
764

Con formato: Fuente: 10 pto

765  
 766  
 767  
 768  
 769  
 770  
 771  
 772  
 773  
 774  
 775  
 776  
 777

**Table 4.** Stable carbon and oxygen isotopes ( $\delta^{13}\text{C}$ ,  $\delta^{18}\text{O}$ ) of samples from the Al Gacel MV and the Northern Pompeia Coral Ridge.

Location	Sample	Origin of the carbonate	Identification number in Fig. 7	$\delta^{18}\text{O}$ (‰)	$\delta^{13}\text{C}$ (‰)
Al Gacel MV	D10-R3	Coral skeleton	1	2.35	-5.58
		Authigenic carbonate	2	3.37	-20.07
			3	3.60	-26.68
			4	3.70	-20.79
			5	3.45	-22.43
			6	3.80	-20.70
		Coral skeleton	7	3.28	-2.23
		Authigenic carbonate	8	3.83	-25.16
			9	3.63	-25.29
			10	3.91	-18.38
			11	3.60	-24.18
			12	3.55	-25.34
			13	3.56	-25.15
		Coral skeleton	14	3.50	-2.09
		Authigenic carbonate	15	3.92	-21.89
	D10-R7	Authigenic carbonate	21	2.90	-26.36
			22	3.15	-28.77
23			2.94	-22.91	
24			2.67	-21.13	
25			2.37	-24.70	
26			2.56	-23.60	
D11-R8	Coral skeleton	16	1.49	-4.91	
		17	2.13	-2.99	

			18	1.74	-4.22
		Authigenic carbonate	19	5.60	-14.82
			20	5.55	-14.74
Northern Pompeia Coral Ridge	D03-B1	Coral skeleton	1.1	-0.38	-7.93
			1.2	-0.86	-7.77
			1.3	-0.51	-7.35
			1.5	1.15	-5.26
			1.4	-1.03	-8.08
			1.6	0.69	-5.96
			1.7	0.54	-6.42

778

779 **Table 4.** Continued

Location	Sample	Origin of the carbonate	Identification number in Fig. 7	$\delta^{18}\text{O}$ (‰)	$\delta^{13}\text{C}$ (‰)
Northern Pompeia Coral Ridge	D03-B1	Coral skeleton	3.1	1.59	-2.08
			3.2	-0.31	-6.27
			3.3	-0.89	-6.78
			3.4	-0.94	-6.73
			3.5	1.84	-2.21
			3.6	2.26	-1.39
			3.7	1.74	-2.87

780

781 **Table 5.** Stable carbon isotopic composition ( $\delta^{13}\text{C}$ ) of selected lipid biomarkers (in **Figure 10**). (\*) Please note  
782 that crocetane in D11-R8 coelutes with phytane. n.d. = not detected.

Compound	D10-R7 (‰)	D11-R8 (‰)
<i>n</i> -C <sub>17</sub>	n.d.	-33.0
<i>n</i> -C <sub>18</sub>	n.d.	-31.8
<i>n</i> -C <sub>19</sub>	n.d.	-31.1
<i>n</i> -C <sub>20</sub>	n.d.	-30.8
<i>n</i> -C <sub>21</sub>	n.d.	-31.5
<i>n</i> -C <sub>22</sub>	n.d.	-31.7
Crocetane*	-101.2	-57.2
PMI	-102.9	-74.3

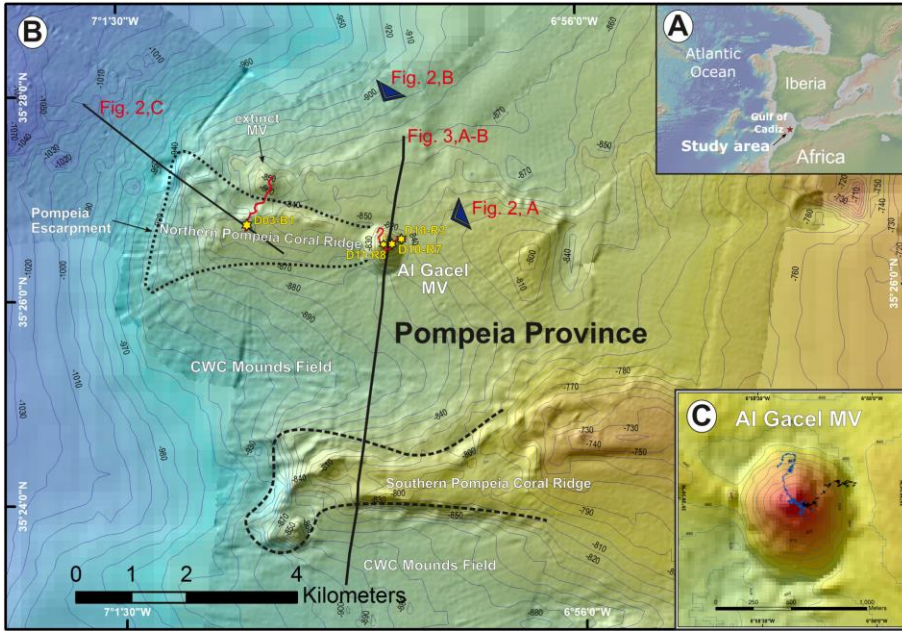
783

784

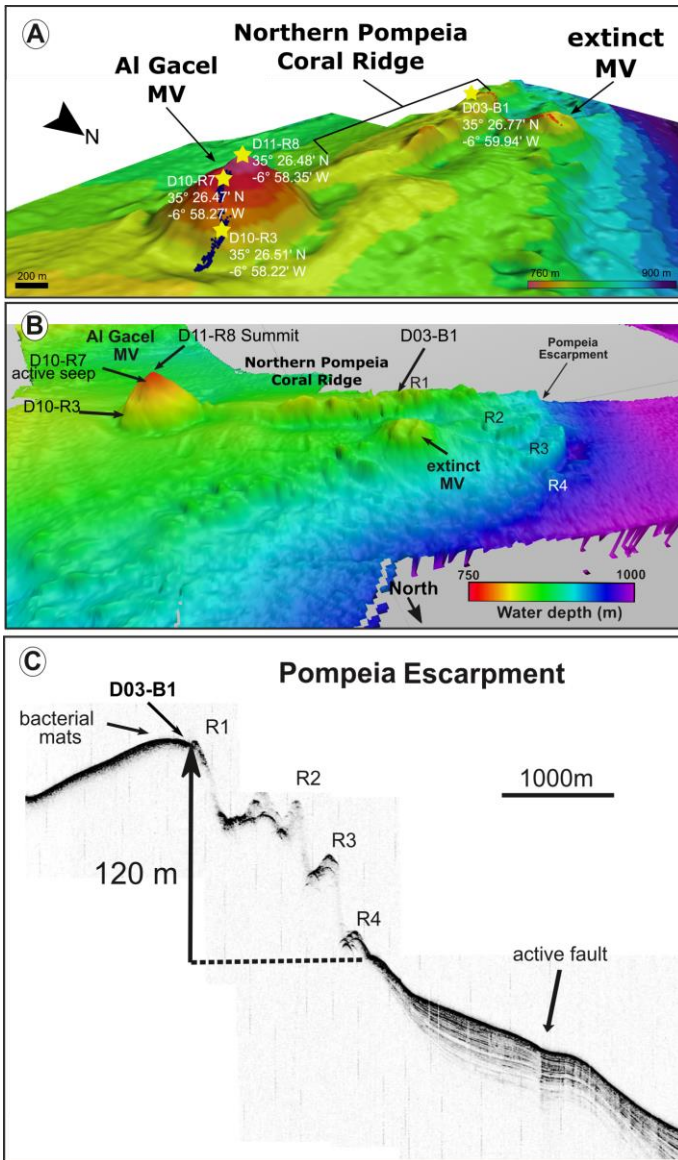
785

|

786  
787  
788  
789  
790  
791

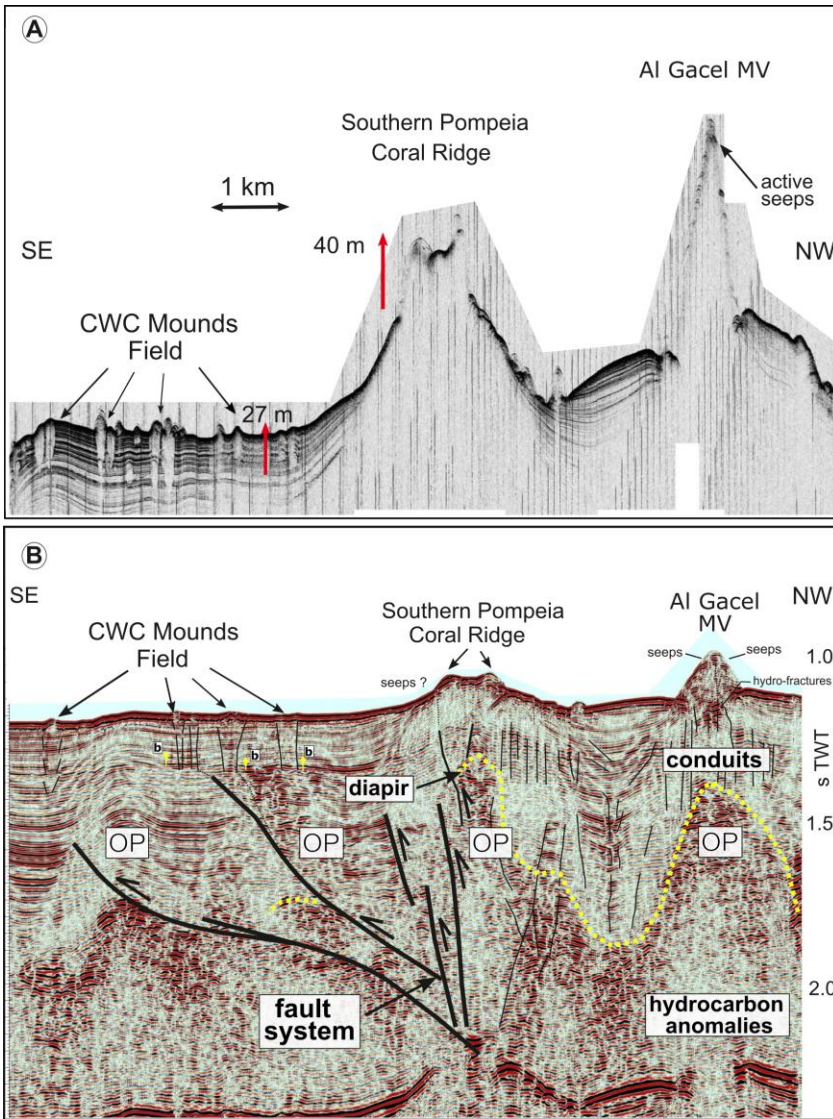


792  
 793 **Figure 1.** Bathymetric map of the study area. **A:** location of the Gulf of Cádiz between Spain, Portugal and  
 794 Morocco. The study area is marked with a red star; **B:** the Pompeia Province including its different morphological  
 795 features. Red lines indicate ROV-paths, yellow stars mark sampling sites; **C:** detailed map of the Al Gacel MV  
 796 including pathways of Dive 10 and 11 (black and blue lines, respectively). Further details of the area are provided  
 797 in **Figs. 2** and **3**.

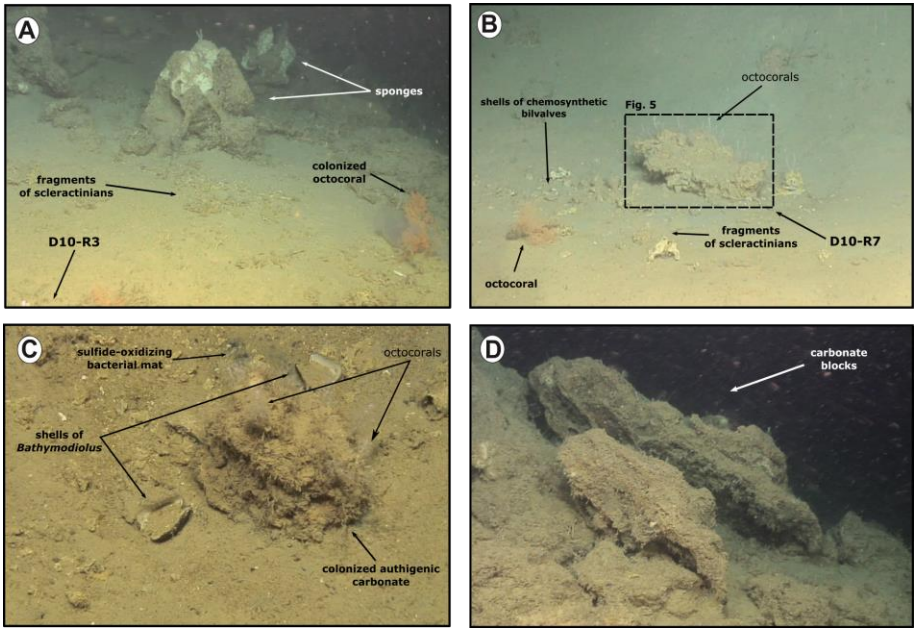


798  
 799 **Figure 2.** Bathymetric and seismic maps showing morphological features in northern Pompeia Province. **A–B:**  
 800 bathymetric maps showing the Al Gacel MV, the Northern Pompeia Coral Ridge and the extinct MV. Yellow stars  
 801 mark sampling sites. **C:** ultra-high seismic profile of the Pompeia Escarpment, westwards of the Northern Pompeia  
 802 Coral Ridge.

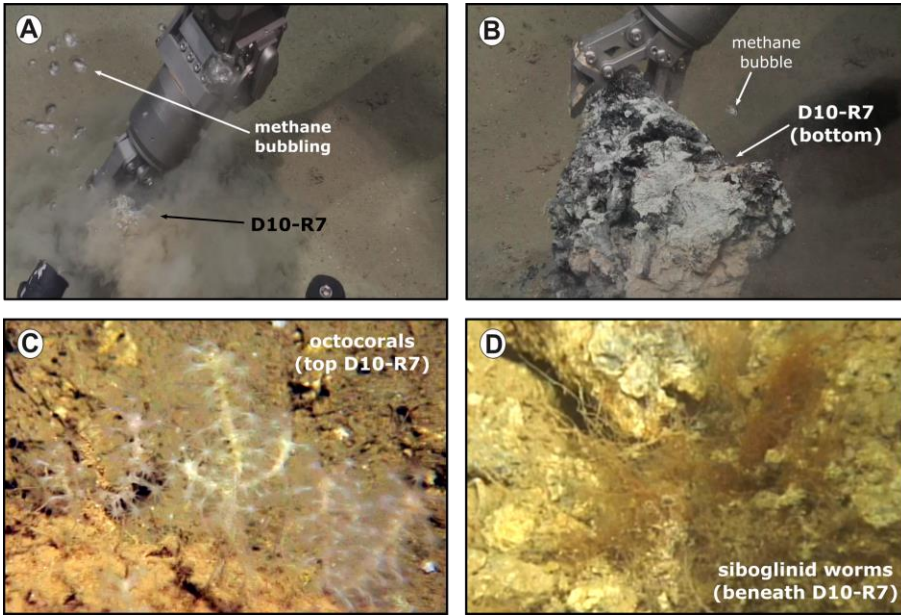
803



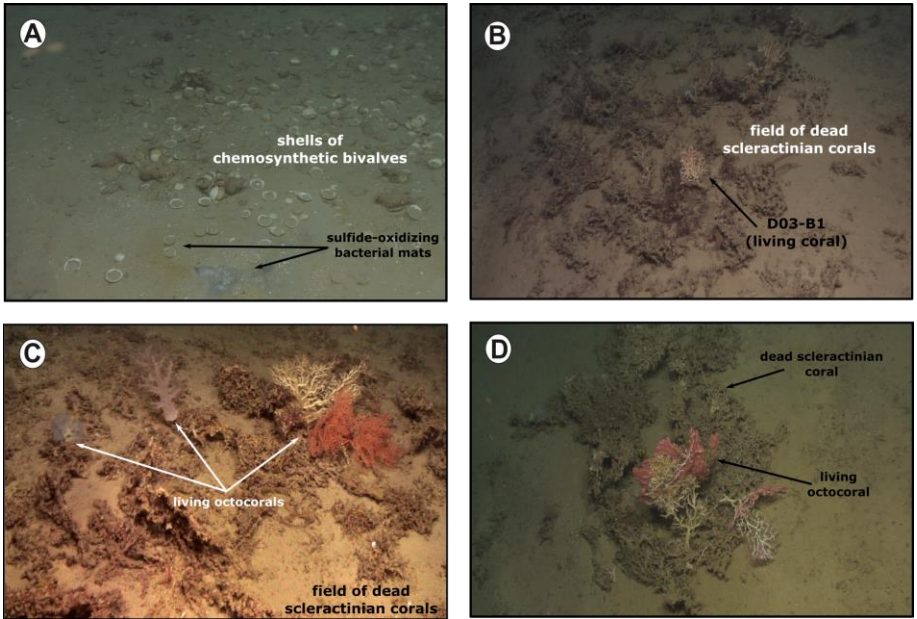
804  
 805 **Figure 3.** Ultra-high resolution (A) and multichannel (B) seismic profiles showing geological features in southern  
 806 Pompeia Province. Note mud diapirism has been described in this area (Vandorpe et al., 2017). OP = overpressure  
 807 zone.



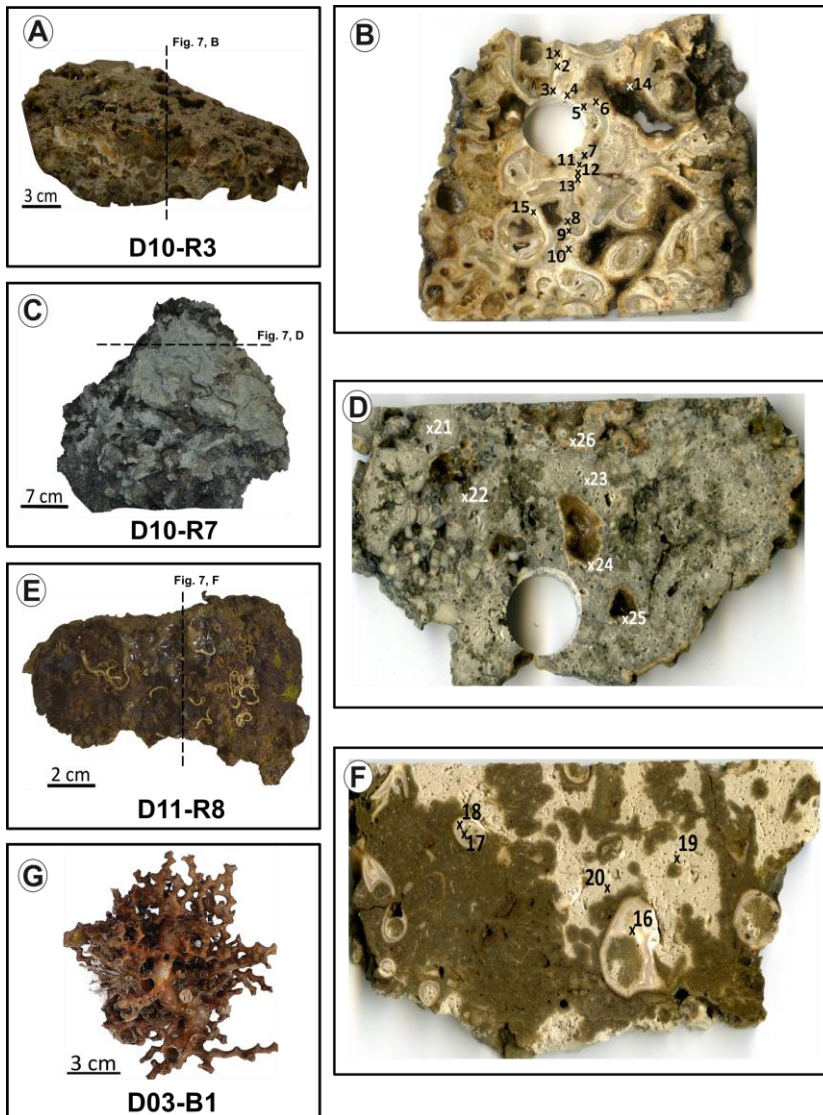
808  
 809 **Figure 4.** ROV still frames from the Al Gacel MV (Dives 10 and 11). **A:** eastern side of the volcano, displaying a  
 810 field of sponges, corals and carbonates; **B–C:** active pockmark sites on the east side of the volcano, displaying  
 811 authigenic carbonate surrounded by shells of chemosynthetic bivalves, fragments of scleractinian and octocorals,  
 812 as well as sulfide-oxidizing bacterial mats; **D:** metric-sized carbonate blocks located in a slope at the summit of  
 813 the volcano.  
 814  
 815



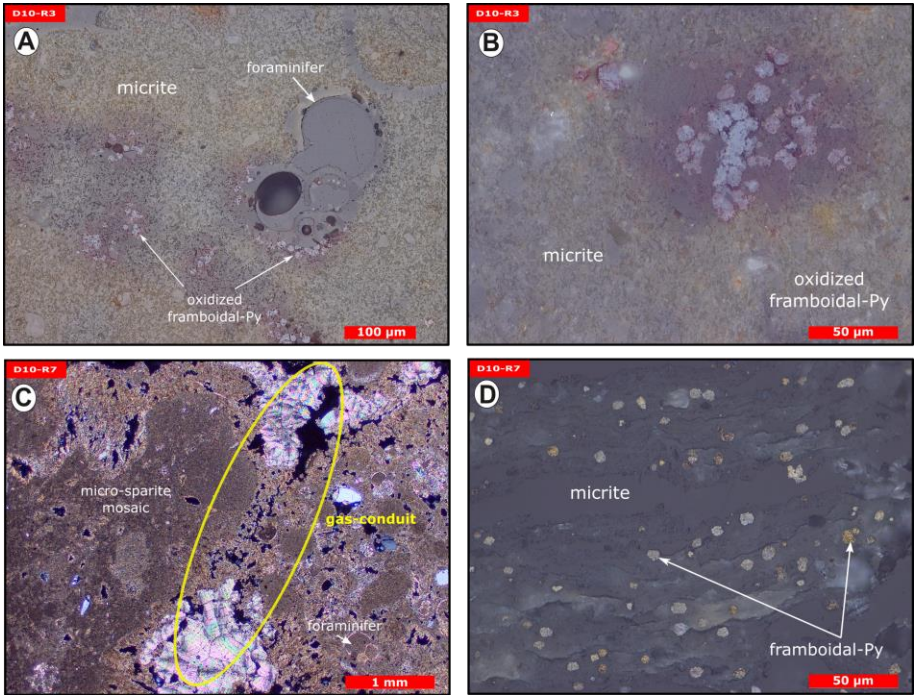
816  
 817 **Figure 5.** ROV still frames from the active pockmark site shown in **Fig. 4, B.** **A–B:** release of bubbles while  
 818 sampling; **C:** detailed photograph of the octocorals on top of the carbonate; **D:** detailed still frame from siboglinid  
 819 worms beneath the carbonate.  
 820  
 821  
 822



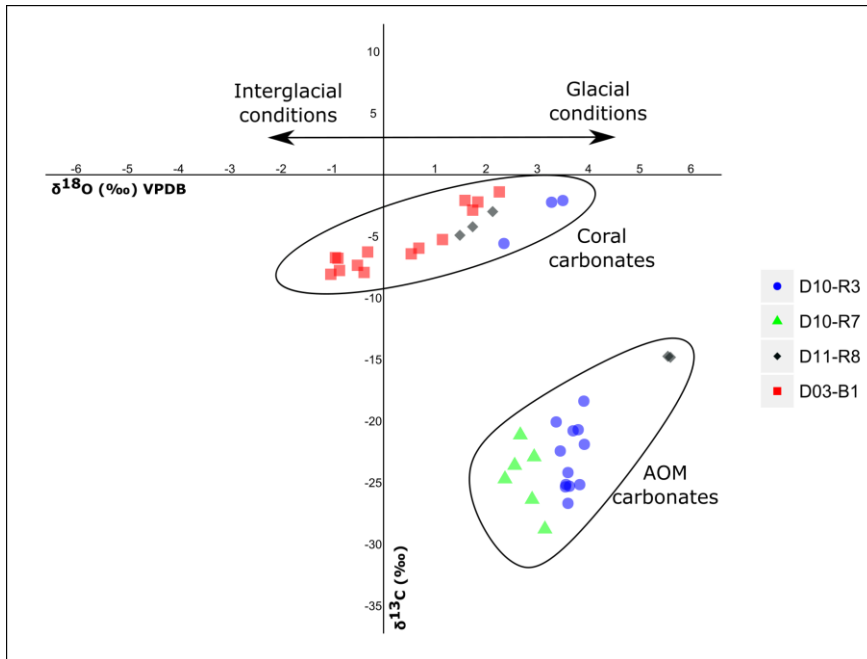
823  
 824 **Figure 6.** ROV still frames from the Northern Pompeia Coral Ridge and extinct MV (Dive 03), where there is  
 825 currently a diffused seepage of fluids. **A:** abundant shells of chemosynthetic bivalves with sulfide-oxidizing  
 826 bacterial mats at the western site of the Northern Pompeia Coral Ridge; **B–D:** field of dead scleractinian-corals  
 827 colonized by living corals; **D:** still frame from the extinct MV.  
 828



829  
 830 **Figure 7.** Photographs of analyzed samples including sampling sites for stable carbon and oxygen isotope ( $\delta^{13}\text{C}$ ,  
 831  $\delta^{18}\text{O}$ ) analysis (crosses with numbers). Values of the stable isotopic analyses are found in **Table 2.** **A–B:** D10-R3  
 832 carbonate with embedded corals; **C–D:** D10-R7 carbonate with strong  $\text{H}_2\text{S}$  odor; **E–F:** D11-R8 carbonate with  
 833 embedded corals; **G:** D03-B1 scleractinian-coral fragment, *Madrepora oculata*. Please note that we cannot  
 834 determine whether the corals were alive or dead the time they were buried by the carbonate.  
 835  
 836  
 837

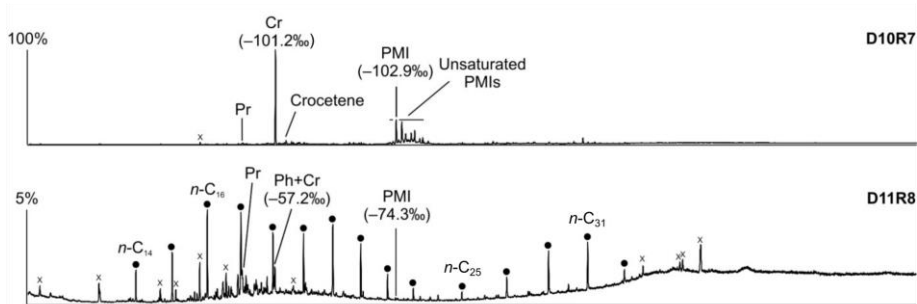


838  
 839 **Figure 8.** Thin section photographs of MDACs. **A–B:** D10-R3 consisting of a micritic matrix with scattered  
 840 foraminifers and oxidized framboidal pyrites (reflected light); **C–D:** D10-R7 consisting of micritic and micro-  
 841 sparitic carbonate with abundant unaltered framboidal pyrites (C, transmitted light; D, reflected light). Please note  
 842 open voids which represent potential pathways for fluid seepage (yellow circle in C).  
 843

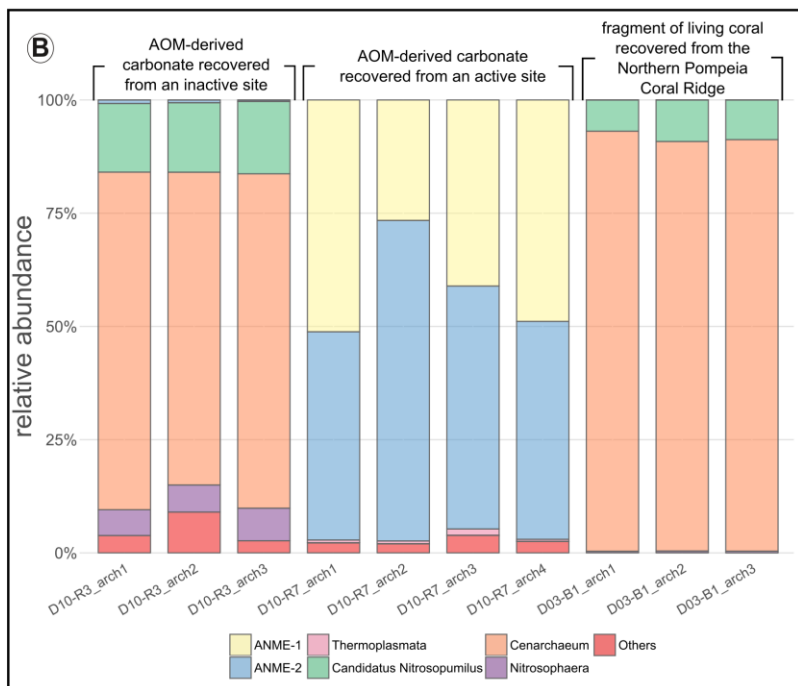
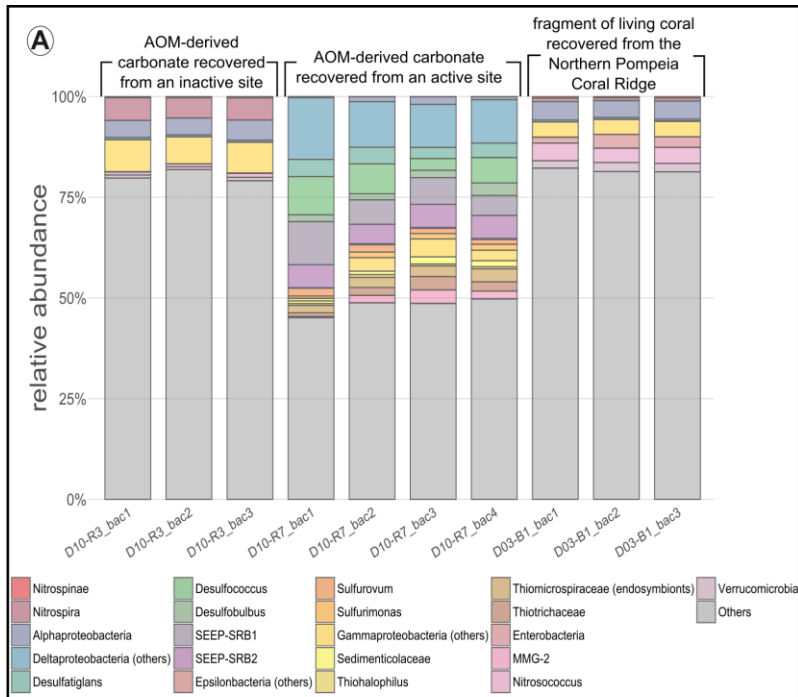


844  
845 **Figure 9.** Stable carbon and oxygen isotopes ( $\delta^{13}\text{C}$ ,  $\delta^{18}\text{O}$ ) of samples from the Al Gacel MV and the Northern  
846 Pompeia Coral Ridge (see **Figure Table 3** and **Fig. 7** for precise sampling points).

Con formato: Fuente: Negrita



851  
852 **Figure 10.** Total ion current (TIC) chromatograms of the analyzed samples. Isotopically depleted acyclic irregular  
853 isoprenoids such as Cr and PMI are typically found in settings influenced by the anaerobic oxidation of methane  
854 (AOM). Pr = pristane; Ph = phytane; Cr = crocetane; PMI = 2,6,10,15,19-pentamethylcosane; dots = n-alkanes;  
855 crosses = siloxanes (septum or column bleeding). Percentage values given on the vertical axes of chromatograms  
856 relate peak intensities to highest peak (Cr in D10-R7).



859 **Figure 11.** Bar chart representing relative abundances of prokaryotic taxa detected in each sample. **A:** bacterial  
860 taxa; **B:** archaeal taxa. In “others” aggrupation is included taxa related to ubiquitous organism normally found in  
861 sea- and seepage-related environments, and unclassified organisms. Number of reads per taxa detailed in **Table**  
862 **S1** (bacteria) and **Table S2** (archaea).

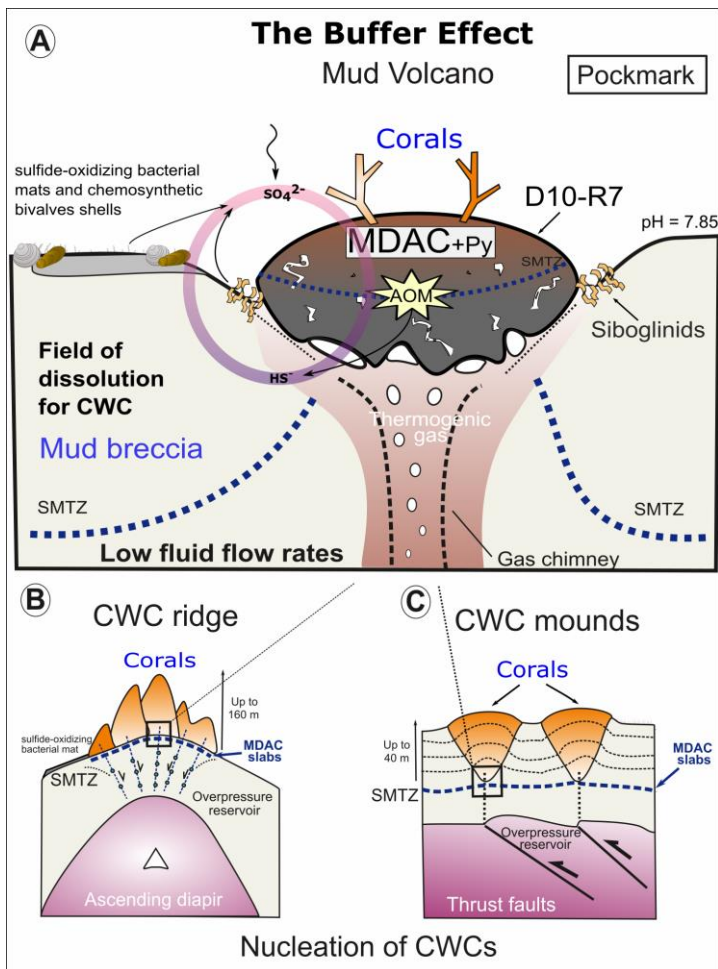


**Figure 12.** The buffer effect model. **A:** Buffer effect at pockmark sites (e.g. sampling site of D10-R7) where carbonates are formed directly on the bubbling site acting as a cap; **B:** Buffer effect at diapiric ridges where MDAC slabs are formed on the base of the ridge; **C:** Buffer effect at coral mounds where MDAC slabs are formed in deeper layers of the sediment. Py = pyrite, SMTZ: sulfur-methane transition zone.

865